

Effect of Mainshock Selection, Earthquake Catalog and Definition on Foreshock Rate Estimates in Southern California



Key Points:

- In Southern California, foreshock rate estimates are sensitive to mainshock selection method, earthquake catalog, and foreshock definition
- Mainshock selection method impacts foreshock rate estimates, because aftershocks of large earthquakes have higher foreshock rates
- Multiple methodological choices produce only minor differences in foreshock rate between standard (20%–23%) and enhanced catalogs (23%–27%)

Supporting Information:

Supporting Information may be found in the online version of this article.

Correspondence to:

R. A. Khan,
russell.azadkhan@bristol.ac.uk

Citation:

Khan, R. A., Werner, M. J., Biggs, J., & Fagereng, Å. (2025). Effect of mainshock selection, earthquake catalog and definition on foreshock rate estimates in Southern California. *Journal of Geophysical Research: Solid Earth*, 130, e2024JB030733. <https://doi.org/10.1029/2024JB030733>

Received 8 NOV 2024

Accepted 17 JUN 2025

Author Contributions:

Conceptualization: R. Azad Khan, M. J. Werner, J. Biggs, Å. Fagereng
Formal analysis: R. Azad Khan
Investigation: R. Azad Khan
Methodology: R. Azad Khan, M. J. Werner, J. Biggs, Å. Fagereng
Project administration: M. J. Werner, J. Biggs, Å. Fagereng
Software: R. Azad Khan
Supervision: M. J. Werner, J. Biggs, Å. Fagereng
Validation: M. J. Werner, J. Biggs, Å. Fagereng
Visualization: R. Azad Khan
Writing – original draft: R. Azad Khan

R. Azad Khan¹ , M. J. Werner¹ , J. Biggs¹ , and Å. Fagereng² 

¹COMET, School of Earth Sciences, University of Bristol, Bristol, UK, ²School of Earth and Environmental Sciences, Cardiff University, Cardiff, UK

Abstract Estimates of the percentage of moderate to large crustal earthquakes (mainshocks) that have foreshocks (the foreshock rate) vary widely: Recent estimates in Southern California using an enhanced catalog range between 19% and 72%. Enhanced catalogs seem to reveal more foreshocks, possibly providing new constraints on nucleation mechanisms, but precise, commonly accepted foreshock definitions are lacking. To investigate the observed range we quantify the sensitivity of foreshock rates to mainshock selection method, catalog (standard and enhanced), foreshock definition, geographical restriction and magnitude cut-offs. We compare two foreshock definitions: Type A—any earthquakes above a magnitude threshold in a space-time window; and type B—an earthquake count in a space-time window that exceeds the 99th percentile of a statistical representation of past seismicity rates (using three distributions: Poisson, Gamma and Empirical). Foreshock rate estimates are increased by (in order of influence): Defining foreshocks using Poisson distributed background rates, using a type A foreshock definition, and removing aftershocks using fixed space-time windows. Rates are lowered by: Removing aftershocks using magnitude-dependent methods, and defining foreshocks using Gamma distributed inter-event times and Empirical distributions of seismicity. A large increase in foreshock rate between the standard and enhanced catalog is only observed when using Poisson distributed background rates for type B foreshocks. A lower magnitude of completeness may thus not lead to significantly more mainshocks with detected foreshocks. Our preferred method, using a more robust mainshock selection and quality-controlled data, estimates ~25% of $M \geq 4$ “mainshocks” in Southern California have foreshocks.

Plain Language Summary Large earthquakes are sometimes preceded by smaller earthquakes (foreshocks), which may reveal the physical processes leading to large earthquakes. Identifying foreshocks in real-time might alert us to impending large earthquakes, potentially enabling short-term warning. Clear, accepted definitions of foreshocks, however, are lacking: Recent studies estimated that between 19% and 72% of large earthquakes in Southern California have foreshocks, each using different methods. Moreover, one study found a large increase in the foreshock rate in an “enhanced” catalog with many more small events, suggesting that foreshocks are detectable before more mainshocks with denser seismic networks and improved methods. In this study, we first recreate and explain this wide range of foreshock rates as a result of different definitions of foreshocks, different mainshock selection methods and several other method choices and data restrictions. Only one combination of choices leads to a large increase in the foreshock rate between the standard and enhanced catalog. Instead, our new preferred method, based on more robust choices, estimates ~25% of mainshocks have foreshocks in the standard and enhanced catalog, respectively. Enhanced catalogs may thus not reveal foreshocks before significantly more mainshocks, placing new constraints on what controls foreshocks and the processes leading to large earthquakes.

1. Introduction

Earthquakes are sometimes preceded by nearby earthquakes which can be referred to as foreshocks. Foreshocks may be a precursory phenomenon that relate to the earthquakes they sometimes precede (Nakatani, 2020), or they may happen by chance (Helmstetter & Sornette, 2003). Currently there is no consensus on the physical mechanism responsible for foreshock generation (Cattania & Segall, 2021; Gomberg, 2018; Ito & Kaneko, 2023; McLaskey, 2019). Similarly, there is no consensus on the definition of a foreshock, for example, how close in space and time an earthquake must precede a mainshock to be labeled a foreshock. Some studies define a

© 2025. The Author(s).

This is an open access article under the terms of the [Creative Commons Attribution License](https://creativecommons.org/licenses/by/4.0/), which permits use, distribution and reproduction in any medium, provided the original work is properly cited.

Writing – review & editing:

R. Azad Khan, M. J. Werner, J. Biggs,
Å. Fagereng

foreshock as any earthquake above a given magnitude (usually set at the completeness magnitude, M_c) within a specific space-time window (Abercrombie & Mori, 1996; Chen & Shearer, 2016; Dodge et al., 1996; Jones & Molnar, 1976; Reasenber, 1999; Wetzler, Brodsky, et al., 2023; Wetzler, Lay, & Brodsky, 2023)—we refer to these as type A foreshocks. There is a long history of type A foreshock studies in Southern California (Abercrombie & Mori, 1996; Chen & Shearer, 2016; Dodge et al., 1996; Jones, 1985; Reasenber, 1999), but improved networks and catalogs (Hauksson et al., 2012; Ross et al., 2019) has enabled more elaborate foreshock analysis, and new foreshock definitions. A string of recent studies have defined foreshocks based on their probability of occurrence according to a statistical representation of the seismicity prior to a mainshock (Moutote et al., 2021; Trugman & Ross, 2019; van den Ende & Ampuero, 2020a)—we refer to these as type B foreshocks. A variety of statistical distributions have been used to define type B foreshocks, including Poisson distributed background rates (Trugman & Ross, 2019), the empirical and Inter-Event Time (IET) distributions (van den Ende & Ampuero, 2020a), and Epidemic Type Aftershock Sequence (ETAS) models (Manganiello et al., 2023; Moutote et al., 2021). We note that some early studies implemented versions of type B foreshock definitions, as they estimated the probability of background events occurring in their space-time windows (Jones, 1984; Jones & Molnar, 1979). The merits of the type A foreshock definition are its simplicity and quick implementation, whilst the merit of the type B definition is that it accounts for foreshock-like sequences that occur but do not lead to mainshocks.

The potential utility of foreshocks in earthquake forecasting is limited by the proportion of mainshocks that have recognizable foreshocks (the foreshock rate), and the false alarm rate. Foreshock rates may vary with region (Wetzler, Brodsky, et al., 2023) and faulting style (Chen & Shearer, 2016; Li et al., 2024; Reasenber, 1999). Recent foreshock rate estimates in Southern California range from 19% to 72% (Moutote et al., 2021; Trugman & Ross, 2019; van den Ende & Ampuero, 2020a; Wetzler, Brodsky, et al., 2023). Three of these studies used type B foreshock definitions (Moutote et al., 2021; Trugman & Ross, 2019; van den Ende & Ampuero, 2020a), and one used type A (Wetzler, Brodsky, et al., 2023). The type A estimates are between 44% and 48% for a range of method choices (Wetzler, Brodsky, et al., 2023). The type B estimates are 19% using an ETAS model to estimate a foreshock window conditional intensity, which is then used as the mean of a Poisson distribution (Moutote et al., 2021); 22% using the empirical distribution (van den Ende & Ampuero, 2020a); 33% using the Gamma distribution (van den Ende & Ampuero, 2020a); and 72% using maximum likelihood estimated background rates (Hainzl, 2006; Van Stiphout et al., 2012) as the mean of a Poisson distribution (Trugman & Ross, 2019). The wide range in foreshock rates therefore seems strongly influenced by the chosen foreshock definition.

Here, we seek to explain the range of reported values and identify a preferred estimate, by considering the following factors that may influence differences in foreshock rate estimates in Southern California:

1. Chosen earthquake catalog: Foreshock rate estimates are expected to be influenced by the magnitude of completeness of the seismic catalog. A catalog with a lower completeness is expected to have a higher foreshock rate. A meta-analysis of type A foreshocks (Mignan, 2015) suggested that foreshocks may only be detectable when there is a three unit difference between the minimum cut-off magnitude (usually set at the completeness magnitude) and mainshock magnitude. Therefore, a catalog with a lower completeness may have a higher proportion of mainshocks with a magnitude three units higher than the cut-off, compared to a higher completeness catalog for the same region. Comparison of foreshock rate estimates between the (standard) Southern California Seismic Network (SCSN) catalog (Hutton et al., 2010) and the (enhanced) Quake Template Matching (QTM) catalogs (Ross et al., 2019) have so far only been made using the foreshock definition from Trugman and Ross (2019), which is thought to overestimate the foreshock rate (Moutote et al., 2021; van den Ende & Ampuero, 2020a). The difference in foreshock rate estimates between the SCSN and QTM catalogs using type A or other type B definitions is currently unknown (see Table 1, which shows all recent foreshock rate estimates in Southern California). Furthermore, the locations of earthquakes can differ between the SCSN and QTM catalogs, as some events in the QTM catalogs have been relocated using the GrowClust algorithm (Trugman & Shearer, 2017). These differences in location could also cause differences in mainshock selection, and foreshock identification.
2. The effect of aftershock sequences of large earthquakes (e.g., the 2010 M7.2 El Mayor-Cucapah earthquake) on mainshock selection. Mainshock selection is important because large, for example, $M \geq 4$, earthquakes that are part of an aftershock sequence will likely be preceded by other earthquakes, and therefore already have a clear cause. Previous foreshock studies using the QTM catalog (Table 1) selected mainshocks by excluding aftershocks using fixed space-time exclusion thresholds, that is, the same threshold regardless of magnitude

Table 1
Recent Foreshock Rate Estimates in Southern California With Method Choices

Study	Foreshock rate (%)	Catalog	Mainshock Selection/Aftershock Exclusion	Mainshock Magnitude Threshold	Number of Mainshocks	Number of Mainshocks w/foreshocks	Foreshock Definition	Minimum Magnitude Cut-off		
T19	48	SCSN	Mag-Dep	4	46	22	Background	None		
	72	QTM 9.5					Poisson			
vdE20	33	QTM 9.5	Mag-Dep	4	46	15	Gamma-IET	None		
	28						Gamma-IET		0.5	
	22						Empirical		None	
M21	20	QTM 9.5	Fixed	4	46	9	ETAS	Local		
	19	QTM 12					Poisson			
W23	48	SCSN	NN	5	35	17	Type A	3		
	44		TMC						40	18
	~64		WnC						30	~19
M23	23–40	HYS	NN and STW	4	143–152	~33–61	ETAS TEST1	2.5		
	9–22						ETAS TEST2			
AK25	35	SCSN, QTMs	Combined (Fixed and Mag-Dep)	4	74	26	type A	3		
	22 (23)	SCSN					16 (17)	Empirical	Both	
	27 (26)	QTM 12					20 (19)	Empirical	Both	
	26 (28)	QTM 9.5					19 (21)	Empirical	Both	
	20 (22)	SCSN					15 (16)	Gamma-IET	Both	
	23 (27)	QTM 12					17 (20)	Gamma-IET	Both	
	23 (30)	QTM 9.5					17 (22)	Gamma-IET	Both	
	46	SCSN					34	Background Poisson	Both	
	51 (58)	QTM 12					38 (43)	Background Poisson	Both	
	51 (61)	QTM 9.5					38 (45)	Background Poisson	Both	

Note. Studies: T19, Trugman and Ross (2019); vdE20, van den Ende and Ampuero (2020a); M21, Moutote et al. (2021); W23, Wetzler, Brodsky, et al. (2023); M23, Manganiello et al. (2023); AK25, this study. Catalogs: SCSN (Hutton et al., 2010), QTM 12 and QTM 9.5 (Ross et al., 2019), and HYS (Hauksson et al., 2011). Mainshock selection/aftershock exclusion methods: Magnitude-Dependent (Mag-Dep) aftershock exclusion (no larger event within magnitude-dependent space-time windows); Fixed aftershock exclusion (no larger event within fixed space-time windows); Combined (both Fixed and Magnitude-Dependent methods); Nearest Neighbor (NN) de-clustering method; WnC (magnitude-varying space and fixed-time windowing); TMC (magnitude-dependent time and space windowing); STW (spatiotemporal windows). Foreshock definitions: Background Poisson (compare foreshock window count to Poisson distributed background rates); Gamma Inter-Event Time (IET) (compare compare foreshock window count to randomly sampled Gamma-distributed inter-event times); Empirical - Empirical Seismicity Rate (compare compare foreshock window count to observed distribution of past seismicity rates); ETAS Poisson (compare foreshock window count to Poisson distributed conditional intensity from an Epidemic Type Aftershock Sequence model); type A ($M \geq 3$ earthquakes); ETAS TEST1 (compare average number of foreshocks to those in ETAS synthetic catalogs); ETAS TEST2 (compare the frequency of foreshocks to those in ETAS synthetic catalogs). The Minimum Magnitude Cut-off column shows whether studies applied a magnitude cut-off: numbers denote a catalog level cut-off, for example, at a magnitude of 3 and above; “Local” denotes a cut-off applied around each mainshock based on the local completeness magnitude; “None” means no cut-off is applied; “Both” means results are calculated with and without a local cut-off. Our study (AK25) focuses on the SCSN and QTM catalogs, the Fixed and Magnitude-Dependent aftershock exclusion methods (Combined), and both type A and B (Background Poisson, Gamma Inter-Event Time and Empirical Seismicity Rate) foreshock definitions. We report two foreshock rate estimates, the first value shows the foreshock rate when we apply a magnitude cut-off, and the second value in brackets without a magnitude cut-off (unless the values are equal in which case a single value is reported). The same is true for the number of mainshocks w/foreshocks column. ~ denotes where exact numbers are not reported or not discernible in publications.

(Moutote et al., 2021), and magnitude-dependent space-time exclusion thresholds (Trugman & Ross, 2019; van den Ende & Ampuero, 2020a). All of these studies excluded the largest earthquake in the catalog, the 2010 M7.2 El Mayor-Cucapah earthquake (Hauksson et al., 2011), due to its location in Mexico, where the network is sparse and the catalog is less complete (see pt.5). Other M7 earthquakes in Southern California, for example, the 1992 Landers, 1999 Hector Mine, and 2019 Ridgecrest earthquakes, occurred outside of the QTM catalog time frame (01 Jan 2008 to 31 Dec 2018). We therefore do not know how recent aftershock exclusion methods

- classify aftershock sequences of $M7+$ earthquakes, or if the fixed and magnitude-dependent methods exclude the same events.
3. **Foreshock definition:** Current type A estimates suggest that nearly half of all mainshocks in Southern California have foreshocks (Wetzler, Brodsky, et al., 2023), whereas the majority of type B estimates range between a fifth and one third (Moutote et al., 2021; van den Ende & Ampuero, 2020a). We acknowledge that Wetzler, Brodsky, et al. (2023) were not pursuing a prediction angle with their foreshock definition, but were using this definition to explore mainshock properties. Higher type A foreshock rates could make this definition more useful in forecasting because it produces more true positives, and is faster and easier to analyze. However, because the type A definition does not consider past seismicity, it may also produce more false positives (earthquakes above the type A threshold that did not lead to mainshocks). The most recent type A foreshock rate estimate (Wetzler, Brodsky, et al., 2023) was for $M \geq 5$ mainshocks from the SCSN catalog (1985–2020), whereas the type B estimates were for $M \geq 4$ mainshocks from 2008 to 2017 in the QTM and/or SCSN catalogs (Table 1). Until we estimate type A and B foreshock rates for the same mainshocks, we cannot tell how strongly the different mainshock magnitude thresholds and timescales may be influencing the differences in rate.
 4. **Magnitude cut-off:** The impact of applying a magnitude cut-off when constructing statistical representations of the seismicity rate for type B foreshock definitions (Moutote et al., 2021; Trugman & Ross, 2019; van den Ende & Ampuero, 2020a) has not been rigorously quantified. One study (vdE20 in Table 1) estimated foreshock rates with and without applying a catalog level magnitude cut-off for one of their two foreshock definitions (van den Ende & Ampuero, 2020a); one study (T19) did not apply a magnitude cut-off at all (Trugman & Ross, 2019); one study (M21) applied a magnitude cut-off based on the local completeness magnitude around mainshocks (Moutote et al., 2021); and two studies (M23 and W23) applied a catalog level magnitude cut-off (Manganiello et al., 2023; Wetzler, Brodsky, et al., 2023).
 5. **Catalog restriction:** no study using type B definitions (Moutote et al., 2021; Trugman & Ross, 2019; van den Ende & Ampuero, 2020a) has estimated foreshock rates for the full QTM catalogs. These studies have only looked inside a subset of the catalog chosen by Trugman and Ross (2019) qualitatively based on spatial completeness and station coverage, which we refer to as the low completeness magnitude region. This region does not include the 2010 $M7.2$ El Mayor-Cucapah earthquake. Including earthquakes outside the low completeness magnitude region increases the number of mainshocks, but requires method adjustments to cope with lower data quality. These method adjustments increase the applicability of our methods to other regions, outside Southern California, which are likely less complete, but important for assessing the influence of a broader range of tectonic settings. Moutote et al. (2021) further restricted their mainshocks to those with ≥ 10 events within 10 km in the past year. The impact of this restriction on foreshock rate estimates is unknown.

In this paper we quantify the impact of different method choices on foreshock rate estimates. We start by quantifying differences in the number of candidate mainshocks ($M \geq 4$ earthquakes from 01 Jan 2009–1 yr after the catalog start date—to 31 Dec 2017) between the SCSN and QTM catalogs, and how location differences between these catalogs affects mainshock selection. We then compare how the Fixed and Magnitude-Dependent aftershock exclusion methods classify aftershocks of the 2010 El Mayor-Cucapah earthquake. Based on these classifications, which include clear aftershocks as mainshocks, we introduce a new Combined method (a combination of the fixed and magnitude-dependent methods), which we use to select a catalog of 74 mainshocks. We estimate the type A and B foreshock rates of these mainshocks in the SCSN and QTM catalogs. We investigate whether the QTM catalog has a significantly higher foreshock rate than the SCSN catalog, using foreshock definitions other than the one used by Trugman and Ross (2019), which defined foreshocks based on abundances relative to Poisson distributed background rates. We also assess the impact of applying a magnitude cut-off, restricting to low completeness magnitude region mainshocks, or to mainshocks with ≥ 10 prior earthquakes. Finally, we discuss the implications of different method choices on foreshock rate estimates, and present our preferred estimates.

1.1. Summary of Previous Foreshock Rate Estimates

Trugman and Ross (2019) found type B foreshocks before 33 of 46 mainshocks (72%) in an enhanced (completeness magnitude $M_c = 0.3$) catalog for Southern California—the QTM catalog (Ross et al., 2019), compared to 22 of 46 mainshocks in a standard ($M_c = 1.7$) monitoring room catalog—the SCSN catalog (Hutton et al., 2010). However, two subsequent studies (Moutote et al., 2021; van den Ende & Ampuero, 2020a) deemed

Table 2

Earthquake Catalogs for Southern California, Giving the Number of Earthquakes in Each Catalog, the Number of Candidate Mainshocks— $M \geq 4$ Events From 01 Jan 2009 (1 yr After the Catalog Start Date) to 31 Dec 2017, the Estimated Completeness Magnitudes M_c (Hutton et al., 2010; Ross et al., 2019), and the Number of Mainshocks We Select After Excluding Aftershocks Using the Fixed, Magnitude-Dependent (Mag-Dep), and Combined Methods

Catalog	Number of earthquakes	Number of candidate mainshocks	M_c	Number of fixed method mainshocks	Number of Mag-Dep method mainshocks	Number of combined method mainshocks
QTM 9.5	1,811,362	276	0.3	125	126	108
QTM 12	898,597	270	0.3	124	124	107
SCSN	179,446	257	1.7	106	108	88
Merged	177,222	248-249 (234)	–	102–103 (96)	102 (98)	85–86 (83)
QTM 9.5 Restricted	1,626,546	93	–	68	67	63
QTM 12 Restricted	791,867	92	–	67	66	62
SCSN Restricted	148,280	90	–	67	64	61

Note. We restrict the SCSN catalog to the time-frame of the QTM catalog (01 Jan 2008 to 31 Dec 2017) to increase comparability. The Merged catalog contains events which are present in the SCSN and QTM catalogs. We report a range in the number of mainshocks selected, as this differs depending on whether we use SCSN or QTM locations. In brackets we report the number of mainshocks with the same selection in both the SCSN and QTM catalogs. The restricted catalogs only contain events inside the low completeness magnitude region, which covers -118.8 to -115.4 in longitude and 32.68 to 36.2 in latitude (see brown box in Figure 1b). We do not report a Merged Restricted catalog as the number of mainshocks inside the low completeness magnitude region changes between the SCSN and QTM catalogs, again due to differences in location.

the 72% foreshock rate estimate in the QTM catalog to be an overestimate. They argued that using background rates in a type B foreshock definition set too low a threshold above which an earthquake count preceding a mainshock is classified as foreshocks. In total, four studies have estimated foreshock rates in Southern California (Manganiello et al., 2023; Moutote et al., 2021; van den Ende & Ampuero, 2020a; Wetzler, Brodsky, et al., 2023) since Trugman and Ross (2019). These four studies did not just use different foreshock definitions, but also varied their mainshock selection methods, choice of earthquake catalog, and whether they applied a magnitude cut-off (all details shown in Table 1). These multiple simultaneous changes make it difficult to know how strongly each of these choices may influence the variations in foreshock rate estimates in Southern California. In total, the five recent foreshock rate estimates in Southern California introduced six mainshock selection methods, four different earthquake catalogs, and six foreshock definitions (Table 1).

2. Data

We use three earthquake catalogs for Southern California (Table 2 and Figure 1): The SCSN catalog (Hutton et al., 2010), and two versions of the QTM catalog (Ross et al., 2019). The estimated completeness magnitudes of the QTM and SCSN catalogs are 0.3 (Ross et al., 2019) and 1.7 (Hutton et al., 2010), respectively. The QTM catalog was created by performing template matching using $\sim 284,000$ earthquake waveforms from the SCSN catalog (2000–2017) (Ross et al., 2019), but the QTM catalog only contains events from 01 Jan 2008 to 31 Dec 2017. To increase comparability we restrict the SCSN catalog to the same time period as the QTM catalogs. Ross et al. (2019) kept the unique identifiers of events they detected through template matching that were already present in the SCSN catalog, and gave new unique identifiers to new events, so events in both catalogs can be easily matched. The two different versions of the QTM catalog (QTM 9.5 and QTM 12) have different event detection thresholds (median absolute deviations of stacked migrated correlation functions of 9.5 and 12). Ross et al. (2019) estimated a 5% false positive rate in the QTM 9.5 catalog, that is, 5% of the earthquakes in this catalog are not real, and a $\leq 1\%$ false positive rate in the QTM 12 catalog. Moutote et al. (2021) found that the QTM 9.5 catalog contains episodic false detections due to processing artifacts, which are not as present in the QTM 12 catalog. The QTM catalogs may be biased because they are inherently more likely to contain newly detected events that are similar to the original waveforms in the SCSN catalog, in particular in areas illuminated by many aftershocks close to the mainshock.

Before we apply mainshock selection methods we consider all $\geq M4$ events that occurred ≥ 1 year after the QTM catalog start date (01 Jan 2008) to be candidate mainshocks, including offshore events. We need this 1 year buffer

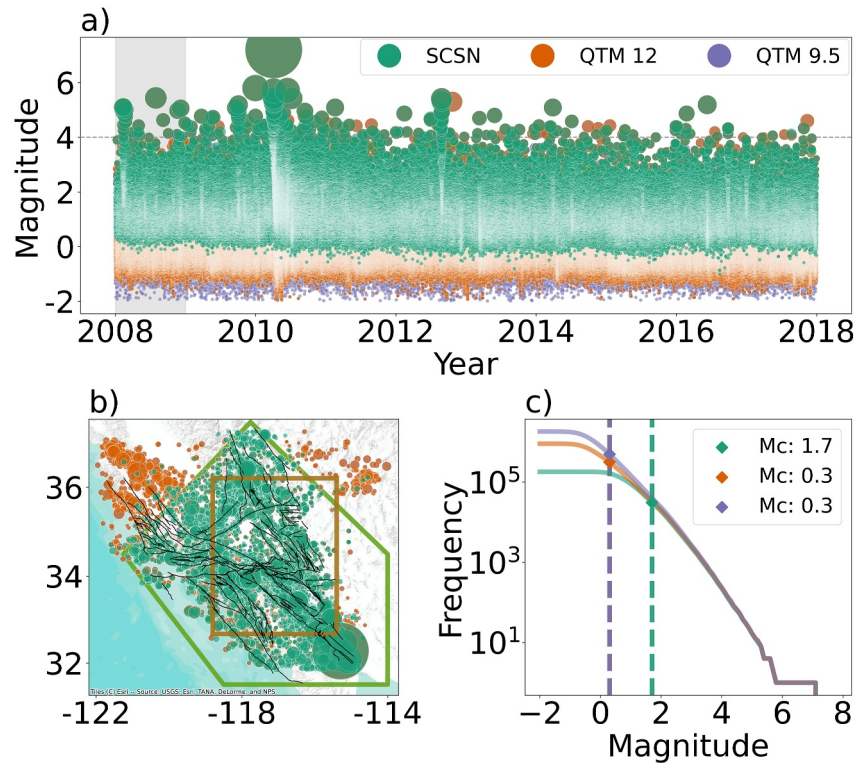


Figure 1. The source parameter data of the earthquake catalogs we analyze. (a) Dots showing magnitudes and times of earthquakes in the SCSN (teal), QTM 12 (orange) and QTM 9.5 (purple) catalogs. Our candidate mainshock magnitude threshold of four is shown by a dashed horizontal gray line, and the period 2008–2009 is grayed out because we do not consider candidate mainshocks during this time. (b) Map of earthquake epicenters shown by dots scaled by magnitude (same scaling as panel a), the low completeness magnitude region is shown by a brown box, and the SCSN reporting region by a green box. The QTM catalogs extend to the northwest and northeast, whereas the SCSN catalog is (mostly) bounded by its reporting region. Black lines show fault data from the SCEC community fault model (Marshall et al., 2023). (c) Catalog Frequency-Magnitude Distributions with completeness magnitude M_c estimates of the QTM catalogs (Ross et al., 2019) and the SCSN catalog (Hutton et al., 2010). The QTM catalogs are an order of magnitude more complete than the SCSN catalog.

so we can check that no larger event occurred in the past year as part of mainshock selection (Section 3.2). There are 13 and 19 more candidate mainshocks in the QTM 12 and QTM 9.5 catalogs, respectively, compared to the SCSN (Table 2). The SCSN catalog is (mostly) bounded by its reporting region (Hutton et al., 2010), whereas the QTM extends to the northwest and northeast of this area (Figure 1b). This difference in catalog extent accounts for most of the additional candidate mainshocks in the QTM versus the SCSN catalogs, as shown by the reduction in this difference for restricted catalogs (Table 2). However, there are still some differences inside of the reporting region, with the QTM catalogs containing two to four (depending on QTM catalog version) more candidate mainshocks inside the low completeness magnitude region than the SCSN catalog. These may be real events found through template matching, which were missed in the SCSN catalog, or they may be false detections.

3. Methods

3.1. Methods Summary

Figure 2 shows the main steps of our workflow. For each of the three earthquake catalogs, we select candidate mainshocks as all events above magnitude four, and then exclude aftershocks using three methods (Section 3.2): a Fixed method, a Magnitude-Dependent method, and a new Combined method (a combination of the Fixed and Magnitude-Dependent methods). These methods exclude candidate mainshocks if they are within the space-time thresholds of a previous larger candidate mainshock, for example, when they are aftershocks. We can then choose to restrict our analysis to low completeness magnitude region mainshocks (Figure 1b), or to mainshocks with ≥ 10 events within 10 km in the past year (Moutote et al., 2021).

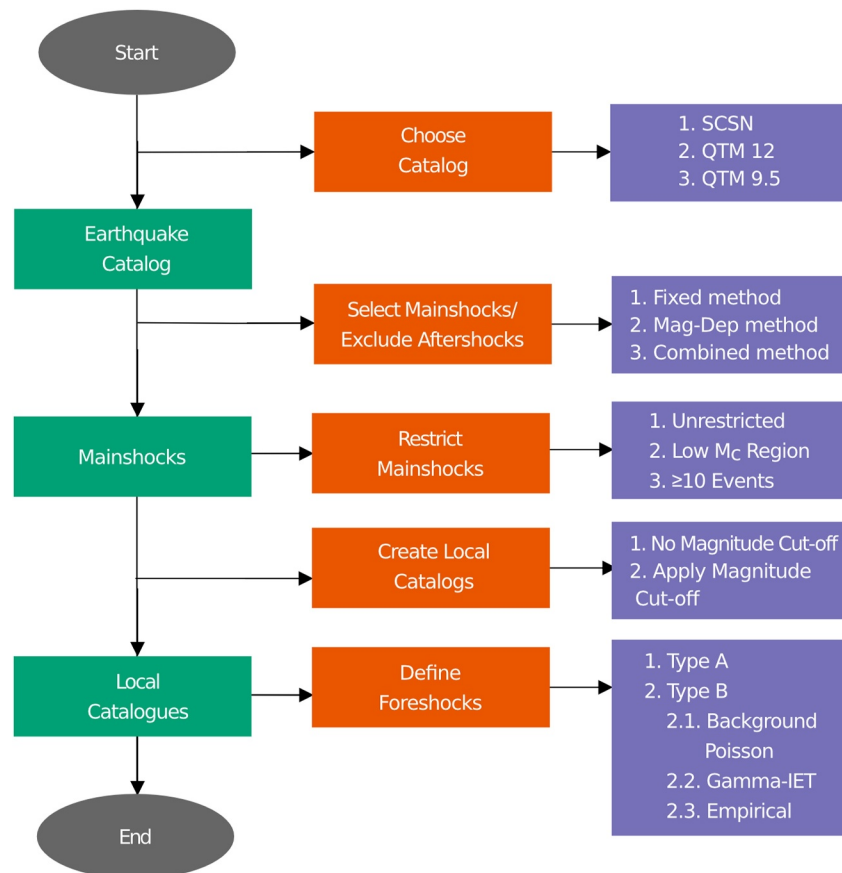


Figure 2. Flow chart of our methodology. Green boxes show data, orange boxes show processes, and purple boxes show decisions.

We create two sets of local catalogs, with and without imposing a magnitude cut-off at the estimated completeness magnitude, comprising events in the past year within 10 km of mainshock epicenters. We use a 10 km radius and 1 year of prior data for our local catalogs for consistency with previous studies (Trugman & Ross, 2019; van den Ende & Ampuero, 2020a). We note that our fixed local catalog radius of 10 km (used for identifying type A and B foreshocks) is different to the exclusion radius of the Magnitude-Dependent aftershock exclusion method (Section 3.2.2). We estimate completeness magnitudes around mainshock epicenters using the b-value stability method (Cao & Gao, 2002). We first select all events within a 10 km radius of mainshock epicenters (the same radius as our local catalogs), however, if we select less than 275 events we expand our search in 5 km increments until we reach this threshold, up to a maximum radius of 50 km. We discard mainshocks which do not meet the 275 event threshold in the SCSN catalog from our final foreshock rate estimates, because we cannot compare the effect of a magnitude cut-off on type B foreshock definitions using these mainshocks, because we cannot robustly estimate completeness magnitudes. We choose 275 as our threshold based on the performance of the b-value stability method (Mignan & Woessner, 2012).

We classify mainshocks as having type A foreshocks if they are preceded by one or more $M \geq 3$ earthquakes within 10 km in the 20-day prior, which we call the foreshock window following the terminology of Moutote et al. (2021). We classify mainshocks as having type B foreshocks if the earthquake count in the foreshock window, N_{obs} , exceeds the 99th percentile of a statistical representation of local catalog seismicity in the period 365 to 20 days prior to mainshocks (the calibration period). We use a type A magnitude threshold of three, a type B calibration period of 365 to 20 days prior to mainshocks, and a type B significance threshold at the 99th percentile for consistency with previous studies (Moutote et al., 2021; Trugman & Ross, 2019; van den Ende & Ampuero, 2020a).

We use three type B foreshock definitions: a Background Poisson - Section 3.3.1 (Trugman & Ross, 2019); a Gamma Inter-Event Time - Section 3.3.2 (van den Ende & Ampuero, 2020a); and an Empirical Seismicity Rate definition—Section 3.3.3 (van den Ende & Ampuero, 2020a). Code for a Gamma Inter-Event Time definition is publicly available (van den Ende & Ampuero, 2020b), but code for the Background Poisson and Empirical Seismicity Rate definitions is not. We integrate the publicly available code and recreate the other methods based on published method descriptions (Trugman & Ross, 2019). We make all the code necessary for our work publicly available (see Open Research Section).

3.2. Mainshock Selection/Aftershock Exclusion Methods

We need to exclude aftershocks from our mainshock catalog, and not just use all events above a magnitude threshold, for example, $M \geq 4$, as aftershocks have a clear cause (the mainshock that triggered them) and will bias the foreshock rate.

3.2.1. Fixed Window Aftershock Exclusion

A Fixed method excludes candidate mainshocks that were preceded by a larger earthquake within a fixed space-time window. Moutote et al. (2021) used a Fixed method with a 20 by 20 km box centered around candidate mainshock epicenters as the space window, and 1 year as the time window. They then further excluded mainshocks that did not have at least 10 earthquakes within these windows (as they needed enough events to perform ETAS inversions). We use a 10 km radius instead which also has a 20 km footprint but avoids corner effects of a box, and is consistent with previous studies which used a radius (Trugman & Ross, 2019; van den Ende & Ampuero, 2020a). We also use a 1-year time window because this ensures that the calibration period does not contain previous larger mainshocks.

3.2.2. Magnitude-Dependent Window Aftershock Exclusion

A Magnitude-Dependent method excludes candidate mainshocks that were preceded by any larger earthquake within magnitude-dependent space-time windows. We calculate these windows for a candidate mainshock, and then exclude subsequent events that are smaller than the candidate mainshock in question. We do this for all candidate mainshocks, even if they have been already excluded, to ensure aftershocks of aftershocks are not included as mainshocks. We use the same window scaling as Trugman and Ross (2019) (Figure 3) with radius $R(M)$ and time-window $T(M)$:

$$R(M) = R_0 + c_R L(M), \quad (1)$$

$$T(M) = T_0 + c_T(M - 4), \quad (2)$$

where $R_0 = 20$ km, $c_R = 5$ km, subsurface rupture length $L = 10^{(M-4.38)/1.49}$ (Wells & Coppersmith, 1994), $T_0 = 50$ days, and $c_T = 25$ days. These are the same parameters as used by Trugman and Ross (2019).

3.2.3. Combined Window Aftershock Exclusion

We define the Combined method as a combination of the Fixed and Magnitude-Dependent methods. We calculate both a fixed and magnitude-dependent space-time window for each candidate mainshock. For a candidate mainshock to be selected, it must not be preceded by anything larger in the past year within 10 km, or within a magnitude-dependent space-time window with a minimum of 20 km and 50 days (Equations 1 and 2). This is shown graphically in Figure 3 for the El Mayor-Cucapah earthquake, as a combination of both the purple and orange boxes. We discuss the merits of the new Combined method in Section 5.1.

3.3. Foreshock Definitions

3.3.1. Background Poisson Definition

We create a Background Poisson definition following Trugman and Ross (2019). A Background Poisson definition quantifies whether a mainshock is preceded by an earthquake count significantly above the background rate (the rate of non-clustered earthquakes). We calculate the background rate by fitting a gamma distribution to the

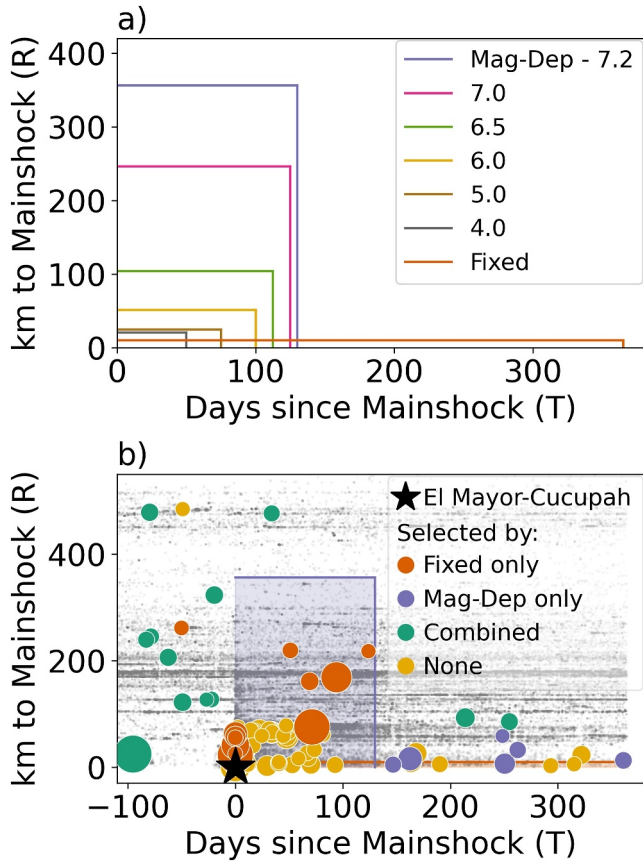


Figure 3. Comparison of the space-time windows of the Fixed and Magnitude-Dependent (Mag-Dep) aftershock exclusion methods. (a) The time T and distance R thresholds of the Magnitude-Dependent method for a range of magnitudes (see key for colors), and the single, magnitude-independent exclusion window of the Fixed method (orange). These methods exclude candidate mainshocks that are within the thresholds of previous larger earthquakes. (b) The time T and distance R thresholds of the methods applied to the El Mayor-Cucupah earthquake (black star), and all seismicity in the QTM 12 catalog (dots) that occurred in the 100 days before and 365 days after within 500 km of the epicenter scaled by magnitude and colored by category. Only the exclusion thresholds for the El Mayor-Cucupah earthquake are shown, but we calculate thresholds for all events (i.e., for aftershocks of El Mayor-Cucupah). Some candidate mainshocks are excluded due to the aftershocks of the El Mayor-Cucupah earthquake, and not by the El Mayor-Cucupah earthquake itself. Dots show candidate mainshocks that are not excluded by either method (i.e., the Combined method), not excluded only by the Fixed method (orange), not excluded only by the Magnitude-Dependent method (purple), excluded by both methods (yellow), and seismicity less than M4 (gray). Mainshocks whose selection/exclusion changes from the SCSN to QTM catalog (due to location differences) are not shown for simplicity.

inter-event time distribution (Hainzl, 2006) using a maximum likelihood estimate (Van Stiphout et al., 2012). The probability density function of a gamma distribution is:

$$P(\tau|\gamma, \mu) = C\tau^{\gamma-1}e^{-\mu\tau}, \quad (3)$$

where τ is the inter-event time variable, γ is the fraction of earthquakes which are mainshocks, μ is the background rate, and C is a normalizing constant equal to $\mu^\gamma/\Gamma(\gamma)$. We estimate γ by minimizing the negative log-likelihood function:

$$\begin{aligned} l &= -\log \text{Likelihood} \\ &= N\gamma \left[1 - \log\left(\frac{N}{T}\gamma\right) \right] + N \log(\Gamma(\gamma)) - \gamma \sum_{i=1}^N \log(\tau_i), \end{aligned} \quad (4)$$

where N is the total number of earthquakes, T is the sum of the inter-event times, and Γ is the gamma function. We can then use γ to estimate the background rate $\mu = N/T * \gamma$. We multiply μ by the time-window $T_w = 20$ days to estimate the typical number of non-clustered earthquakes in a 20-day period. We then use this as the mean (λ) of a Poisson distribution (Equation 5), which represents the probability of seeing a number of earthquakes n in 20 days:

$$P(n|\lambda) = \frac{\lambda^n e^{-\lambda}}{n!}, \quad (5)$$

The probability of observing the foreshock window earthquake count N_{obs} or greater is given by:

$$P(n \geq N_{obs}) = 1 - \sum_{k=0}^{N_{obs}-1} \frac{\lambda^k e^{-\lambda}}{k!}. \quad (6)$$

3.3.2. Gamma Inter-Event Time Definition

A Gamma Inter-Event Time definition can quantify whether a mainshock is preceded by an earthquake count significantly above expected earthquake counts, based on random sampling of independent inter-event times. We construct a Gamma Inter-Event Time definition using the publicly available code from van den Ende and Ampuero (2020b). Firstly, this code fits a gamma distribution to the IET distribution (τ) using the Scipy.Stats.Gamma function:

$$P(\tau|\alpha, \beta) = \frac{\beta^\alpha \tau^{\alpha-1} e^{-\beta\tau}}{\Gamma(\alpha)}, \quad (7)$$

where α is the shape parameter, β the scale parameter, and Γ is the gamma function. The code then generates 200 random samples from the fitted gamma distribution (τ_2). The first sample, $\tau_2[i = 0]$, is then multiplied by a random number between zero and one, resulting in T_0 . τ_2 is then cumulatively summed, and negatively shifted by T_0 . The code then counts how many values in τ_2 are more than t_{win} (20 days). If no values are more than t_{win} , 200 more samples are drawn (τ_3), and the process is repeated until at least one value lies outside t_{win} . The number of values within t_{win} is then counted (n). We note that the original code from van den Ende and Ampuero (2020b) subtracted one from this count, but we opt not to subtract one as by shifting the first event, the sampled inter-event times do not start with an event, and so

there is no need to subtract one. This final count represents how many earthquakes could be seen in a 20-day period according to this representation. This whole process is repeated 50,000 times, so that there are 50,000 values of n (representing 50,000 possible 20-day earthquake counts). The code then fits another gamma distribution to values of $n > 0$:

$$P(n|\alpha_2, \beta_2) = \frac{\beta_2^{\alpha_2} n^{\alpha_2-1} e^{-\beta_2 n}}{\Gamma(\alpha_2)}, \quad (8)$$

where the subscript 2 denotes that the parameters are different to those in Equation 7. This gamma distribution (Equation 8) represents the probability of observing integer earthquake counts per 20 days, whereas the previous gamma distribution (Equation 7) represents the likelihood of observing inter-event times (τ) as a continuous random variable. The probability of observing an earthquake count n equal to N_{obs} or greater is given by:

$$P(n \geq N_{obs}) = 1 - \sum_{k=0}^{N_{obs}-1} \frac{\beta_2^{\alpha_2} k^{\alpha_2-1} e^{-\beta_2 k}}{\Gamma(\alpha_2)}. \quad (9)$$

In the original code from van den Ende and Ampuero (2020b), if all events lie outside t_{win} (giving a count of zero), subtracting one gives a count of -1 , which is nonphysical. The original code excludes these negative counts by only fitting the final gamma distribution to counts where $n > 0$ (which is necessary as the gamma function is defined only for $n > 0$). However, the probability of quiescence (zero earthquakes in 20 days) therefore cannot be represented by this foreshock definition.

3.3.3. Empirical Seismicity Rate Definition

An Empirical Seismicity Rate definition can quantify whether a mainshock is preceded by an earthquake count significantly above past observed earthquake counts (van den Ende and Ampuero, 2020a). We construct an Empirical Seismicity Rate definition by moving a 20-day sliding window with a 0.01 days increment across local catalog earthquakes in the calibration period, counting the number of earthquakes in each window (32,500 windows in total). The counts then form a nonparametric distribution representing the probability of seeing a number of earthquakes n in 20 days. The probability of observing an earthquake count n equal to N_{obs} or greater is given by:

$$P(n \geq N_{obs}) = 1 - \sum_{k=0}^{N_{obs}-1} P(k), \quad (10)$$

where $P(k) = N_k/N_{samples}$ where N_k is the number of samples which equal k , and $N_{samples}$ is the total number of samples (32,500). Our method differs from the original (van den Ende & Ampuero, 2020a) method which generated 50,000 uniform points across the calibration period, and then took the 20-day earthquake counts at each of these points. We instead use the sliding window described above because it is computationally less expensive, and gives identical foreshock rate estimate results for the 46 mainshocks analyzed by van den Ende and Ampuero (2020a). We note that a 0.01 days increment is very small, and the earthquake counts in these windows will be highly dependent (because the windows overlap, the counts in adjacent windows contain mostly the same earthquakes, i.e., they are not independent), but we use this increment so our results are comparable to the original study by van den Ende and Ampuero (2020a).

3.4. Local Catalogs With ≤ 10 Events

Some mainshocks outside the low completeness magnitude region are preceded by too few calibration period (365 to 20 days prior) events to fit gamma distributions to the inter-event time distribution, which is required to create the Background Poisson and Gamma Inter-Event Time type B definitions (Sections 3.3.1 and 3.3.2). Rather than excluding these mainshocks for example, by setting a 10 prior event requirement like Moutote et al. (2021), we introduce the following steps to classify these mainshocks as having or not having type B foreshocks. Mainshocks preceded by zero earthquakes in the foreshock window (20 to 0 days prior) are considered not to have foreshocks. Mainshocks preceded by ≥ 1 earthquake in the foreshock window and zero earthquakes in the

calibration period are deemed to have foreshocks. Mainshocks for which we are unable to create the Background Poisson or Gamma Inter-Event Time definitions have foreshocks if the number of earthquakes in the foreshock window is greater than the number of earthquakes in the calibration period, and do not have foreshocks if the opposite is true. We set this strict requirement (of requiring more observed earthquakes in the foreshock window than in the entire calibration period) because we do not want to artificially inflate our foreshock rate results by including mainshocks in areas of poor data quality/network detection.

4. Results

In this section, we first investigate differences in the number of candidate mainshocks in the SCSN and QTM catalogs (Table 2). We next investigate how mainshocks selection changes between the SCSN and QTM catalogs due to location differences. Thereafter we analyze how the Fixed and Magnitude-Dependent aftershock exclusion methods classify aftershocks of the El Mayor-Cucapah earthquake. Subsequently we calculate the impact of mainshock selection methods on foreshock rate estimates. We move forward with a catalog of 74 mainshocks we select after applying the Combined aftershock exclusion method. These mainshocks are present in both the SCSN and QTM catalogs, their selection does not change between these catalogs due to location differences, and they have completeness magnitudes estimated using ≥ 275 events. We use these mainshocks to compare foreshock rate estimates using type A ($M \geq 3$ earthquakes in foreshock windows) and B (high earthquake counts in foreshock windows relative to past counts) methods in the SCSN and QTM catalogs. We finally assess the impact on foreshock rate estimates of restricting to: (a) low completeness magnitude region mainshocks; (b) mainshocks with ≥ 10 prior earthquakes; and (c) applying a magnitude cut-off to type B foreshock definitions.

4.1. Mainshock Selection

There are 257 candidate mainshocks ($M \geq 4$ events from 01 Jan 2009 to 31 Dec 2018) in the SCSN catalog, 270 in the QTM 12, and 276 in the QTM 12 (Table 2). There are 248 candidate mainshocks common to all three catalogs (Figure 4a). 28 candidate mainshocks are present in the QTM catalogs which are not in the SCSN catalog (Figure 4a) of which 21 are outside the SCSN reporting region, and seven are inside (Figures 4b and 4c). There are nine candidate mainshocks in the SCSN which are not in the QTM catalogs (Figure 4a). Eight of these mainshocks are in the southeast (Figure 4c), with the remaining mainshock in the north (Figure 4b). We note that although the SCSN reporting region includes the El Mayor-Cucapah sequence (pink box in Figures 4c and 5a), it is technically located south of the border in Mexico, so the network coverage is not as good. This likely explains why there are larger discrepancies between catalogs in this area. We exclude mainshocks not present in both the QTM and SCSN catalogs, because we cannot compare differences in foreshock identification between catalogs for these mainshocks.

Candidate mainshock locations can change between the SCSN and QTM catalogs (Figure S1 in Supporting Information S1), which causes the selection of 14 mainshocks to change between the catalogs (Figure 5). All 14 of these mainshocks are located in the area of the El Mayor-Cucapah earthquake, with one occurring in the year before, and 13 occurring in the 2 years after. We restrict our study to mainshocks whose selection does not change between the SCSN and QTM catalogs (Figures 6a and 6c). We refer to this as our merged catalog.

In our merged catalog (events present in all three catalogs) we select (i.e., do not exclude as aftershocks) 83 mainshocks using our Combined method. There are 28 mainshocks selected only by the Fixed or Magnitude-dependent methods: 13 Fixed-only and 15 Mag-Dep-only (Figures 6a and 6c). 123 candidate mainshocks are selected by none of the methods, with 93 of these occurring in the year after the El Mayor-Cucapah earthquake. A mainshock selected only by the Fixed method must be within the Magnitude-Dependent exclusion thresholds of a larger event, and is therefore deemed an aftershock by the Magnitude-Dependent method. A mainshock selected only by the Magnitude-Dependent method must be within the Fixed exclusion thresholds of a larger event, and is deemed an aftershock by the Fixed method. Of the 13 Fixed-only mainshocks, seven occur within 1 year and 50 km of the El Mayor-Cucapah epicenter (Figures 6b and 6d), with the other six similarly close to other events, suggesting these events are likely aftershocks. All 15 Magnitude-Dependent-only mainshocks are preceded by a larger event within 10 km in the past year, suggesting also that these are aftershocks. Twelve occur after the El Mayor-Cucapah earthquake and within 100 km of the epicenter (6 visible in the year after in Figures 6b and 6d), whilst the other three are similarly close to other events. We thus exclude the 28 candidate mainshocks selected only by the Fixed or Magnitude-Dependent methods from our final foreshock rate estimates.

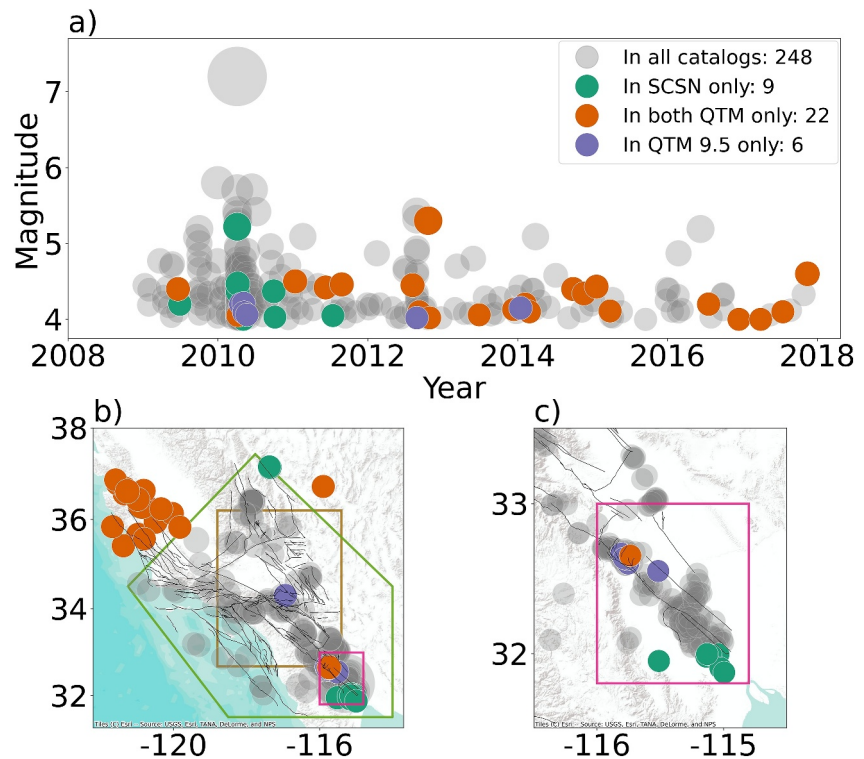


Figure 4. The times, magnitudes, and locations of candidate mainshocks in the SCSN, QTM 12 and QTM 9.5 catalogs, colored by the catalog(s) in which events are present: Events present in all three catalogs (transparent gray); events only in the SCSN (teal), events in both QTM catalogs but not the SCSN (orange); and events only in the QTM 9.5 (purple). The number of candidate mainshocks changes between catalogs. (a) Candidate mainshock times and magnitudes. (b) Candidate mainshock locations. A green box denotes the SCSN reporting region, a brown box the low completeness magnitude region, and a pink box the area of the El Mayor-Cucapah earthquake. (c) A zoom in of panel b, better showing the difference in candidate mainshocks between catalogs around the area of the El Mayor-Cucapah earthquake.

4.2. Example Mainshock

Figure 7 shows, for an example mainshock (ID 37301704, M 4.25, 04 Jan 2015) using SCSN and QTM 12 data, the local catalog data, the distributions for type B foreshock definitions (illustrated using both probability density and cumulative distribution functions) and their 99th percentiles, and the foreshock window with a log timescale. This mainshock does not have type B foreshocks (Empirical Seismicity Rate or Gamma Inter-Event Time definitions) in the SCSN catalog (Figure 7c), but does in the QTM 12 catalog (Figure 7d) for both the Empirical Seismicity Rate and Gamma Inter-Event Time definitions. There is only one other mainshock (Figure S2 in Supporting Information S1—ID: 11006189) which does not have foreshocks in the SCSN, but does then have foreshocks in the QTM 12 for both the Empirical Seismicity Rate and Gamma Inter-Event Time definitions. When we apply a magnitude cut-off at the local completeness magnitude, mainshock ID37301704 still flips from not having to having foreshocks in the SCSN versus QTM 12, whereas mainshock ID11006189 no longer flips.

The Background Poisson definition deems mainshock ID37301704 to have foreshocks in both the SCSN and QTM catalogs. This is because the Background Poisson definition reaches significance ($p < 0.01$) with fewer events than the Gamma Inter-Event Time and Empirical Seismicity Rate definitions (Figures 7c–7f). This behavior of the Background Poisson definition is the reason it gives higher foreshock rate estimates than other methods, as already shown by van den Ende and Ampuero (2020a). The significance thresholds of the Gamma Inter-Event Time and Empirical Seismicity Rate models are more similar, with the Gamma Inter-Event Time definition having a higher threshold than the Empirical Seismicity Rate definition in the SCSN catalog, but a marginally lower threshold in the QTM 12. We note that the Background Poisson and Empirical Seismicity Rate PDFs give a similarly high probability of observing quiescence (zero earthquakes), whilst the Gamma Inter-Event Time definition gives a probability of zero. This is true in both the SCSN and QTM 12 catalogs.

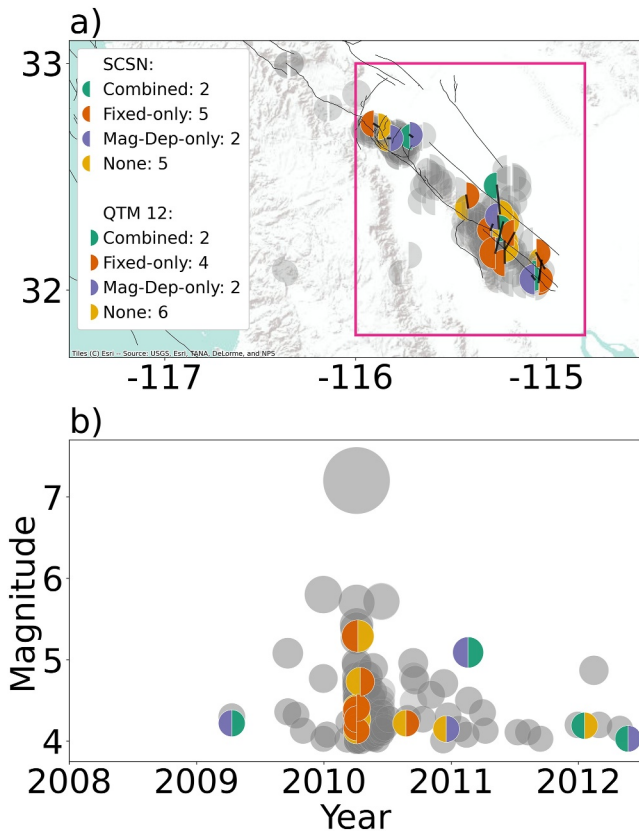


Figure 5. Mainshock selection results for candidate mainshocks present in all catalogs in the region of the El Mayor-Cuapah earthquake. Events whose selection does not change between the catalogs are shown in gray, whilst events whose selection does change are colored by their selection (see key). Half circles with left fill denote selections and locations of events in the SCSN catalog, and half circles with right fill the QTM 12 catalog. (a) Locations of candidate mainshocks, with a black line joining locations in the SCSN and QTM catalogs. (b) Magnitudes and times of candidate mainshocks.

Our example mainshock only has 34 events within 10 km in the past year in the SCSN, but has 280 events within 15 km (which is above our requirement of 275), and so we estimate $M_c = 1.2$ for this mainshock using the 280 events within 15 km. However, there are nine mainshocks out of the 83 Combined selected mainshocks (from our merged catalog) for which we cannot robustly estimate completeness magnitudes, because they were preceded by fewer than 275 events within 50 km (Figure S3 in Supporting Information S1). All nine mainshocks are located offshore, where there are significantly fewer seismic stations. We exclude these nine mainshocks, and note that this does not significantly alter the foreshock rate estimates (Section S3 in Supporting Information S1). This leaves 74 mainshocks with which we can estimate foreshock rates in the SCSN and QTM catalogs, with and without a magnitude cut-off set at the local completeness magnitude.

4.3. Foreshock Rate Estimate Comparisons

We only observe a large increase in foreshock rate estimates from the SCSN to QTM catalogs for the Background Poisson definition without a magnitude cut-off (Figure 8). Nine and 11 out of 74 mainshocks go from not having foreshocks in the SCSN, to having foreshocks in the QTM 12 and QTM 9.5 (respectively), for the Background Poisson definition without a magnitude cut-off (all results in our study are shown in Table 1). When we apply a magnitude cut-off, only 4 mainshocks go from not having foreshocks in the SCSN, to having foreshocks in the QTM catalogs, for the Background Poisson definition. For the Empirical Seismicity Rate and Gamma Inter-Event Time definitions, with or without applying a magnitude cut-off, only two to six mainshocks go from not having foreshocks in the SCSN to having foreshocks in the QTM catalogs. Only two mainshocks change state for both the Empirical Seismicity Rate and Gamma Inter-Event Time definitions (Figure 7 and Figure S2 in Supporting Information S1), however, this reduces to one when we apply a magnitude cutoff. When we apply restrictions (≥ 10 prior events or low completeness magnitude region) the increases in foreshock rate from the SCSN to QTM catalogs are proportionally larger (Figures 8b and 8c), but still only due to between two and six mainshocks changing status (for the Empirical Seismicity Rate and Gamma Inter-Event Time definitions). Applying a magnitude cut-off generally decreases the differences in estimates between the catalogs, especially for the Background Poisson definition.

For unrestricted mainshocks (Figure 8a) the type A ($M \geq 3$ earthquakes in foreshock windows) foreshock rate estimate is 35% (26/74 mainshocks). Type A estimates slightly decrease inside the low completeness magnitude region to 33% (16/49 mainshocks) (Figure 8b), but increase to 42% (22/53 mainshocks) when we restrict to mainshocks preceded by ≥ 10 events (Figure 8b), compared to with no restrictions. Type A estimates are in closer agreement with the Empirical Seismicity Rate and Gamma Inter-Event Time estimates inside the low completeness magnitude region (Figure 8c), but sit $\sim 10\%$ – 15% above them for unrestricted mainshocks, and for mainshocks preceded by ≥ 10 events (Figures 8a and 8b). Type A estimates are always significantly below Background Poisson estimates. There is no change between catalogs for type A foreshock rate estimates (Figure 8) because the SCSN and QTM catalogs are similar from M3 and above (Figure 1c). There is also no change in type A estimates when we apply a magnitude cut-off, as all the catalogs are complete below M3 (Figure 1).

Restricting to mainshocks with ≥ 10 events in the past year (Figure 8b), or low completeness magnitude region mainshocks increases foreshock rate estimates by $\sim 0\%$ – 15% depending on the definition (Figure 8c). Although the foreshock rate is lower when we do not apply restrictions (i.e., proportionally fewer mainshocks outside of restriction areas have foreshocks), we can identify more mainshocks with foreshocks in total. For the Empirical Seismicity Rate definition, we identify up to five more mainshocks with foreshocks, and for type A foreshocks we

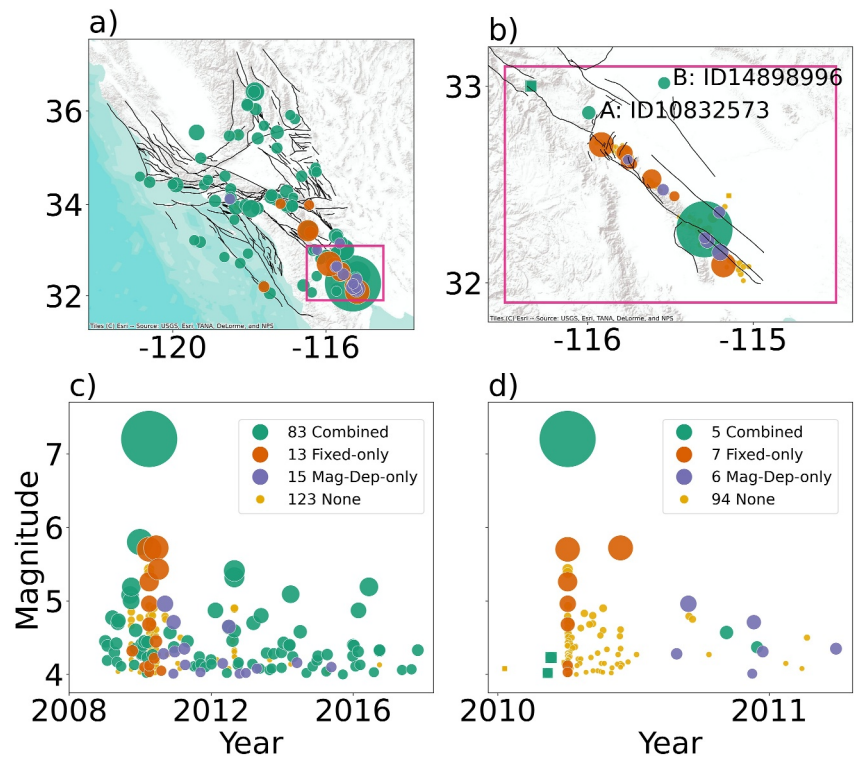


Figure 6. Locations and times of events in our merged catalog (events present in all three catalogs) scaled by magnitude. (a) Map of all mainshocks (dots), colored by selection method (see key in panel c), using QTM 12 locations. Combined denotes events selected by both the Fixed and Magnitude-Dependent methods (Section 3.2). The pink box shows the region of the 2010 M7.2 El Mayor-Cucapah earthquake. (b) Zoom in on the pink box of panel a but restricted to events 4 months before to 1 year after the El Mayor-Cucapah earthquake. (c) Times and magnitudes of earthquakes from panel a. (d) Times and magnitudes of earthquakes from panel b. The Fixed and Magnitude-Dependent methods select some clear aftershocks of the El Mayor-Cucapah earthquake as mainshocks. Two mainshocks selected by the Combined method which occur prior to the El Mayor-Cucapah earthquake are shown as squares (panels b and d). Two mainshocks selected by the Combined method after the El Mayor-Cucapah earthquake are labeled (panel b).

identify up to 10 extra, compared to if we applied restrictions. This is useful to maximize the number of mainshocks with foreshocks available to analyze.

Figure 9 shows the impact of including the 28 mainshocks selected only by the Fixed or Magnitude-Dependent methods on foreshock rate estimates (Section 4.1). In general, Fixed-only mainshocks (Figure 9b) have higher foreshock rate estimates than Combined mainshocks (Figure 9a), and Magnitude-Dependent-only mainshocks have lower foreshock rate estimates, except for type A (Figure 9c). Type A estimates are significantly higher for both Fixed-only and Magnitude-Dependent-only mainshocks, compared to Combined mainshocks.

4.4. Do Type A and B Foreshocks Occur Together?

In the QTM 12 catalog, 94% of mainshocks with type B foreshocks (according to all of the Background Poisson, Gamma Inter-Event Time, and Empirical Seismicity Rate definitions, with a magnitude cut-off) also have type A ($M \geq 3$ earthquakes in foreshock windows) foreshocks (15/16 mainshocks), but only 58% of mainshocks with type A foreshocks also have type B foreshocks (15/26 mainshocks). Figure 10 illustrates the co-occurrence of type A and B foreshocks in the QTM 12 catalog (with a magnitude cut-off applied). 16 of the 74 mainshocks have type B foreshocks according to all definitions (Background Poisson, Gamma Inter-Event Time, and Empirical Seismicity Rate - pink stars), with 15 of these also having type A foreshocks (pink stars with black outlines). 26 mainshocks have type A foreshocks (all stars with black outlines), and 58% of these also have type B foreshocks (15/26) according to all definitions (pink stars with black outlines). This leaves 11 mainshocks with type A foreshocks but not type B. Of these, four do not have type B foreshocks according to any definition (brown stars

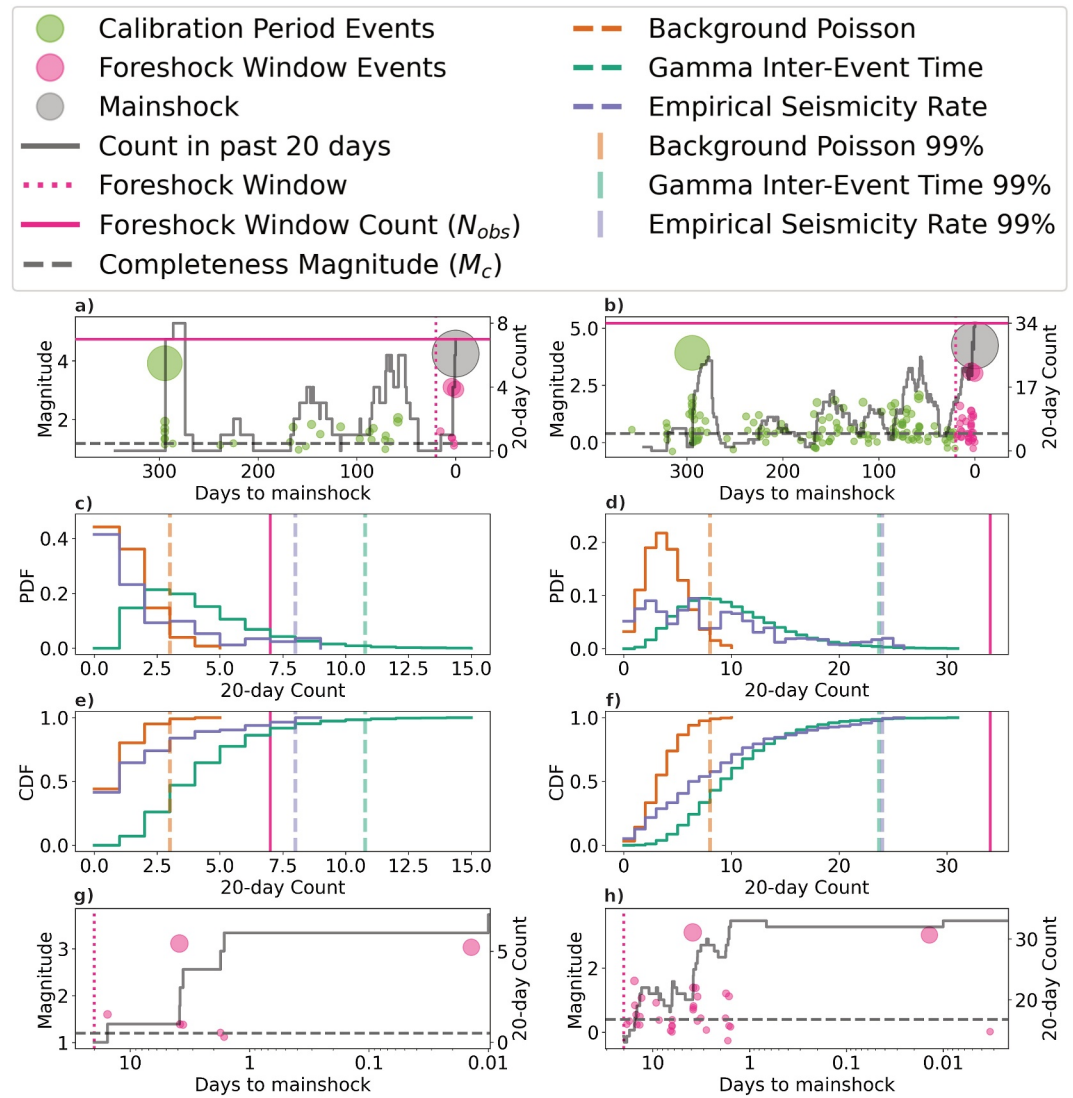


Figure 7. Illustrative foreshock analysis for an example mainshock (ID 37301704, M 4.25, 04 Jan 2015) from the SCSN (left column) and QTM 12 catalog (right column), without applying a magnitude cut-off. (a, b) Magnitudes and times of local catalog events (see key) scaled by magnitude. A stepped gray line shows the earthquake count in the past 20 days. A solid horizontal pink line shows N_{obs} —the earthquake count in the foreshock window (which starts at the dotted vertical pink line 20 days before the mainshock). A dashed horizontal gray line shows the estimated completeness magnitude. (c, d) Probability Distribution Functions (PDFs) of 20-day earthquake counts during the calibration period, using the Background Poisson (orange), Gamma Inter-Event Time (IET, teal), and the Empirical Seismicity Rate (Empirical, purple) representations. The vertical dashed colored lines show the 99th percentiles of each PDF. A vertical pink line shows N_{obs} . A definition deems the mainshock to have foreshocks if N_{obs} is to the right of the 99th percentile. (e, f) The cumulative distribution functions (CDFs) of the type B definitions with the same key and color as panels c and d. (g, h) A zoom in of panels a and b showing only the foreshock window, note the logarithmic time scale on the x-axis. This mainshock is not classified as having type B foreshocks according to the Empirical Seismicity Rate and Gamma Inter-Event Time definitions in the SCSN, but is classified as having type B foreshocks in the QTM 12 catalog by both the Empirical Seismicity Rate and Gamma Inter-Event Time definitions.

with black outlines), and seven have type B foreshocks according to at least one but not all definitions (green stars with black outlines).

For these results, the Empirical Seismicity Rate and Gamma Inter-Event Time definitions agree on 16 mainshocks, with five mainshocks only having foreshocks according to one of these definitions (one for Gamma Inter-Event Time definition, and four for the Empirical Seismicity Rate definition). Three of these five mainshocks

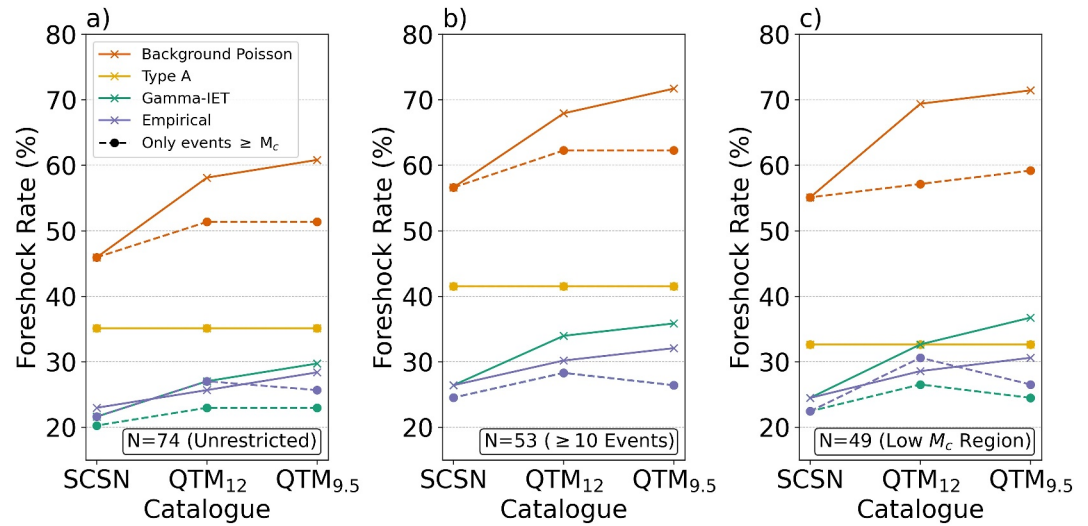


Figure 8. Foreshock rates estimated using four foreshock definitions (type A, Empirical (Seismicity Rate), Gamma Inter-Event Time (IET), and Background Poisson), and three catalogs (SCSN, QTM 12, and QTM 9.5), with and without a magnitude cut-off (circles and dashed lines vs. and crosses and solid lines, respectively). (a) Our merged mainshock catalog ($n = 74$). (b) Restricting to mainshocks with ≥ 10 events in the past year ($n = 53$). Note, the Gamma Inter-Event Time and Empirical Seismicity Rate definitions with a magnitude cut-off give the same result for this restriction. (c) Restricting to low completeness magnitude (M_c) region mainshocks (brown box in Figure 4b) ($n = 49$). We observe similar foreshock rate estimates in the SCSN and QTM catalogs for all definitions except the Background Poisson definition, which shows a marked increase.

have type A foreshocks. We note that the Gamma Inter-Event Time definition thresholds are higher than the Empirical Seismicity Rate thresholds 62% of the time ($n = 46$). For 14% of mainshocks ($n = 10$) we were unable to create the Gamma Inter-Event Time distribution due to insufficient data, and therefore we set thresholds based on our assumptions (Section 3.4). Only one of these 10 mainshocks has foreshocks (ID: 37506472), as there were

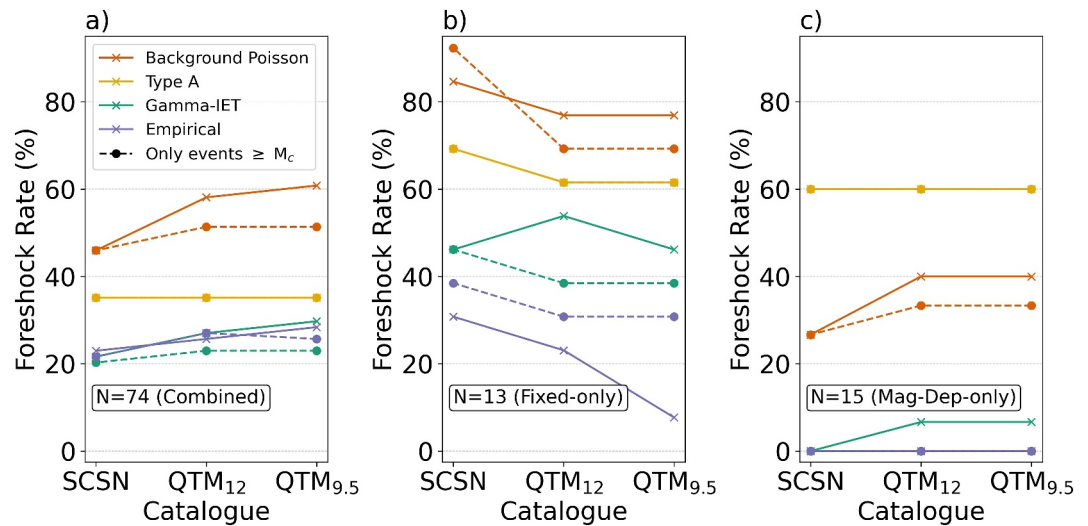


Figure 9. Foreshock rate estimates for different mainshock selection methods (Combined, Fixed-only, Magnitude-Dependent-only) in the SCSN, QTM 12, and QTM 9.5 catalogs, color coded by foreshock definition. (a) 74 mainshocks selected by the Combined method; (b) 13 mainshocks only selected by the Fixed method; (c) 15 mainshocks selected only by the Magnitude-Dependent method. The results show that Fixed-only mainshocks generally have higher type A and B foreshock rate estimates than Combined mainshocks, and Magnitude-Dependent-only mainshocks have higher type A but lower type B foreshock rate estimates than Combined mainshocks.

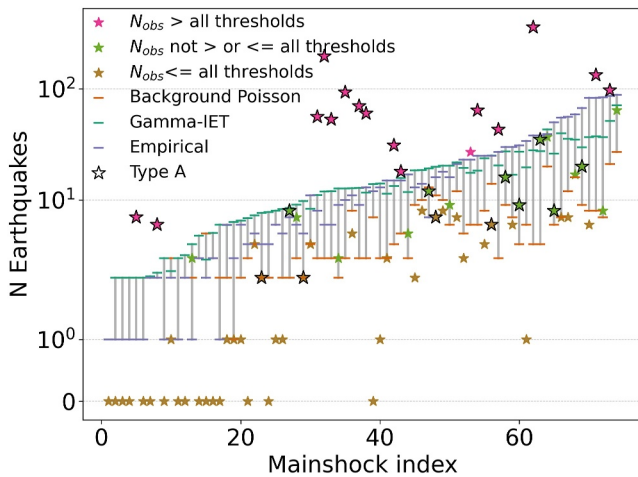


Figure 10. The 99th percentiles of the type B foreshock definition Probability Density Functions (PDFs) (Background Poisson—orange, Gamma Inter-Event Time (IET)—teal, Empirical (Seismicity Rate): purple) for mainshocks from our merged catalog (using QTM 12 data, with a magnitude cut-off applied). Colored stars mark the earthquake count in the foreshock window (N_{obs}) before each mainshock. Pink stars denote mainshocks for which $N_{\text{obs}} >$ the 99th percentile of all PDFs. Brown stars denote mainshocks for which $N_{\text{obs}} <$ the 99th percentile of all PDFs. Green stars denote mainshocks for which N_{obs} is in between the 99th percentiles of the PDFs. Stars with black outlines denote mainshocks with type A foreshocks. 94% of mainshocks with type B foreshocks (according to all of the Background Poisson, Gamma Inter-Event Time, and Empirical Seismicity Rate definitions, with a magnitude cut-off) also have type A foreshocks (15/16 mainshocks), but only 58% of mainshocks with type A foreshocks also have type B foreshocks (15/26 mainshocks). Some mainshocks at lower indexes only have two 99th percentiles visible. These are mainshocks for which we could not fit a Gamma distribution to the inter-event time distribution because of too few events (Section 3.4), and so we set thresholds based on assumptions. The Gamma-Inter-Event Time and Background Poisson thresholds are the same for these mainshocks (and therefore plot on top of each other).

5.1. Mainshock Selection

Our study is the first to analyze in detail how recent mainshock selection methods treat aftershocks of a major ($M > 7$) earthquake, specifically, the 2010 M7.2 El Mayor-Cucapah earthquake (Figure 3b). Future applications of the methods, either in different regions or over different time windows, should reasonably avoid selecting aftershocks of major earthquakes. The Fixed (Moutote et al., 2021) and Magnitude-Dependent (Trugman & Ross, 2019) methods both select some aftershocks of the El Mayor-Cucapah earthquake as mainshocks (Figure 6), and including these mainshocks can strongly impact (typically increase) foreshock rate estimates (Figure 9). Fixed-only mainshocks have higher type A ($M \geq 3$ earthquakes in foreshock windows) and B (high earthquake counts in foreshock windows relative to past counts) foreshock rate estimates (Figure 9b) due to aftershocks of previous larger events in their foreshock windows. Fixed-only mainshocks are more likely to have aftershocks in the foreshock window because they can be preceded by a larger event at any time, as long as it is further than 10 km away. Magnitude-Dependent-only mainshocks, however, have lower type B foreshock rate estimates due to aftershocks of previous larger events in their calibration periods. This raises the threshold for type B foreshock definitions, meaning a higher earthquake count in the foreshock window is required for these mainshocks to have type B foreshocks. This causes lower foreshock rate estimates, except for type A (Figure 9c). Type A foreshock rate estimates for Magnitude-Dependent-only mainshocks are higher than Combined mainshocks. The type A foreshock definition does not consider past seismicity and so a lower type A rate is not expected for Magnitude-Dependent-only mainshocks, as with type B.

seven events in the foreshock window and only two events in the calibration period. This mainshock also has type A foreshocks ($n = 2$ $M \geq 3$ events), both of which occurred ~ 1 day prior to the mainshock.

5. Discussion

Our key findings are as follows: (a) The Fixed and Magnitude-Dependent mainshock selection methods both select some aftershocks of the 2010 M7.2 El Mayor-Cucapah earthquake as mainshocks, and including these aftershocks as mainshocks can strongly impact foreshock rate estimates. (b) The type B (high earthquake counts in foreshock windows relative to past counts) Background Poisson definition gives very high foreshock rate estimates compared to all other definitions (type A or B), because of its low threshold for foreshock classification, as previously noted by van den Ende and Ampuero (2020a). (c) For type B definitions other than the Background Poisson (i.e., the Empirical Seismicity Rate and Gamma Inter-Event Time definitions), with or without a magnitude cut-off, we estimate only slightly higher foreshock rates in the QTM catalogs (23%–30%), compared to the SCSN catalog (20%–23%) (Table 1 and Figure 8). This contradicts the previously found increase from 48% to 72% (Trugman & Ross, 2019). (d) We estimate lower type A ($M \geq 3$ earthquakes in foreshock windows) foreshock rates for $M \geq 4$ mainshocks (35%) than previously found for $M \geq 5$ mainshocks (44%–48%) (Wetzler, Brodsky, et al., 2023), but they are still higher than all of our type B estimates for Empirical Seismicity Rate and Gamma Inter-Event Time definitions (20%–30%), which are similar to previous estimates for the same definitions (van den Ende and Ampuero (2020a). We now discuss: Why Fixed-only and Magnitude-Dependent-only mainshocks have higher foreshock rates, and whether the Combined mainshock selection method is a suitable alternative (Section 5.1); how our foreshock rate estimates in the SCSN and QTM catalogs compare to previous estimates, and what our results say about finding foreshocks before more mainshocks in enhanced catalogs (Section 5.2); the potential utility of type A and B foreshocks in earthquake forecasting (Section 5.3); the limitations of our study (Section 5.4); and our preferred methods and estimates of foreshock rates in Southern California (Section 5.5).

We combine the Fixed and Magnitude-Dependent mainshock selection methods to construct the Combined method, which by design excludes the aftershocks of the 2010 El Mayor-Cucapah earthquake which the Fixed or Magnitude-Dependent method deems mainshocks (Figure 6d). We note that two Combined mainshocks (Figure 6b) occur within 1 year of the El Mayor-Cucapah earthquake, but because these events are located off of the main rupture (A and B in Figure 6d) we view their inclusion by the Combined method as reasonable. We therefore propose the Combined method as a more suitable mainshock selection method for future foreshock studies, especially in regions with large earthquakes. The parameters we use for the Combined method are the same as the studies which introduced the Fixed and Magnitude-Dependent methods (Moutote et al., 2021; Trugman & Ross, 2019), but more optimal parameters may exist. We show that aftershocks selected as mainshocks are much more likely to have foreshocks than mainshocks which are not part of an aftershock sequence (Figure 9). Including these events as mainshocks may therefore inflate foreshock rate estimates.

We note that our Fixed and Magnitude-Dependent methods select a different number of mainshocks compared to what is reported in the original papers (for the same catalogs, in the same region, over the same time period). Details of how the mainshocks our Fixed and Magnitude-Dependent methods select compare to previous studies (Moutote et al., 2021; Trugman & Ross, 2019) can be found in Section S5 in Supporting Information S1.

5.2. SCSN Versus QTM

This is the first study to compare foreshock rate estimates of the same mainshocks in the SCSN and QTM catalogs other than Trugman and Ross (2019), who did so using only the Background Poisson definition, without applying a magnitude cut-off. Trugman and Ross (2019) reported a 50% increase in foreshock rate estimates, from 48% in the SCSN (22/46 mainshocks), to 72% in the QTM 9.5 (33/46). These 46 mainshocks were selected using the Magnitude-Dependent method in the low completeness magnitude region. Since then, it has been demonstrated that the Background Poisson definition overestimates foreshock rates (van den Ende and Ampuero (2020a), which our results support (Figures 7 and 8). Our results therefore provide a much needed update on whether using the QTM catalogs gives higher foreshock rate estimates than the SCSN catalog. When we look at type B definitions other than the Background Poisson definition (i.e., the Empirical Seismicity Rate and Gamma Inter-Event Time definitions), we observe only minor increases in foreshock rate estimates in the SCSN to QTM catalogs (Figure 8). We observe a similar trend when we restrict to mainshocks with ≥ 10 events in the past year, or to mainshocks in the low completeness magnitude region, but the proportional increases are larger (Figures 8b and 8c). Although an increase exists, it is only caused by 2–6 of 74 mainshocks going from not having foreshocks in the SCSN, to having foreshocks in the QTM catalogs. Of these, only two mainshocks change their foreshock classification according to both the Empirical Seismicity Rate and Gamma Inter-Event Time definitions (Figure 7 and Figure S2 in Supporting Information S1), the other four are either one or the other but not both. Furthermore, this reduces to one mainshock when we apply a magnitude cut-off (Figure 7). Our results therefore suggest that the increase in type B foreshock rate estimates between the SCSN and QTM catalogs, if any exists, is small, and probably not significant.

Despite the QTM catalogs reportedly being over one unit magnitude more complete than the SCSN (Hutton et al., 2010; Ross et al., 2019) (Figure 1), this is not the case for a significant proportion of local catalogs around mainshock epicenters (Figure S4, S5 in Supporting Information S1). For 72% of mainshocks we estimate a completeness magnitude of QTM 12 local catalogs that is within ± 0.25 units of our estimated completeness magnitude of SCSN local catalogs (Figure S4a, S4b in Supporting Information S1). Of these, 11% have an increased completeness magnitude in the QTM 12, 31% have the same completeness magnitude, and 30% show a decrease (of < 0.25 units). This leaves 28% of mainshocks which show a decreased completeness magnitude in the QTM versus the SCSN of more than 0.25 magnitude units. There are significantly more local catalog events (in the past year) in the QTM than the SCSN (Figure S4c, S4d in Supporting Information S1), however the number of events above completeness is broadly similar (Figure S4e, S4f in Supporting Information S1). 76% of mainshocks are preceded by within ± 30 events above completeness in the year prior in the QTM versus the SCSN catalog. This illustrates that the improvement in the bulk completeness magnitude of the QTM does not necessarily hold in particular sub-datasets of interest, such as the foreshock windows studied here.

Comparing foreshock rate estimates for a mainshock in the SCSN and QTM catalogs with a magnitude cut-off is redundant if the local catalog has a similar completeness magnitude and event count above completeness. Not applying a magnitude cut-off gives the QTM catalogs the greatest opportunity to reveal enhanced foreshock

activity, at the risk of introducing detection bias. However, even without a magnitude cut-off we do not find a substantial increase in foreshock rate estimates between the SCSN and QTM catalogs, using definitions other than the Background Poisson (Figure 8). Furthermore, when we restrict to the 28% of mainshocks ($n = 21$) with a completeness magnitude decrease of ≥ 0.25 in the QTM 12 (vs. the SCSN), we do not see a significant increase in foreshock rate estimates (SCSN-6/21 and QTM 12-7/21 mainshocks with Empirical Seismicity Rate foreshocks with a magnitude cutoff). Our results therefore temper the hypothesis that we see (type B) foreshocks before more mainshocks as the catalog completeness magnitude decreases (Mignan, 2015). However, it may be that the QTM is not enhanced enough to investigate this, and that an enhanced catalog with more regions with a significantly decreased completeness magnitude would be more suitable. Regardless, our results suggest that a substantially greater effort in further catalog enhancement would be required to evidence a significant increase in foreshock rates.

5.3. Type A Versus B

Our study is the first to compare type A ($M \geq 3$ earthquakes in foreshock windows) and B (high earthquake counts in foreshock windows relative to past counts) foreshock rates using the same mainshocks (Table 1). Our type B foreshock rate estimates (Figure 8a -Empirical Seismicity Rate: 22%–28%; Gamma Inter-Event Time: 20%–30%) are similar to previous estimates (Empirical Seismicity Rate: 22%; Gamma Inter-Event Time: 33%) made by van den Ende and Ampuero (2020a), but for 28 more mainshocks. Our type A estimates of 35% are lower than the previous 44%–48% estimate (Wetzler, Brodsky, et al., 2023), but are for a different time-frame of the SCSN catalog, a different mainshock selection method, and $M \geq 4$ mainshocks, not $M \geq 5$ (Table 1).

To allow comparison between studies using different thresholds, classic papers on foreshock rate estimates reported the foreshock rate per magnitude unit difference between the mainshock magnitude threshold and the minimum magnitude cut-off (also termed foreshock rate density). Most studies estimated the foreshock rate density to be between 12% and 17% (Abercrombie & Mori, 1996; Agnew & Jones, 1991; Chen & Shearer, 2016; Jones, 1984; Jones & Molnar, 1979; Reasenber, 1999). We can roughly estimate our foreshock rate density, if we use the completeness magnitudes of the SCSN (1.7) and QTM (0.3) catalogs as our minimum magnitudes (Figure 1c). Using the Empirical Seismicity Rate definition we obtain a foreshock rate density of 10% using the SCSN catalog, and 8% using the QTM 12 catalog. Although lower than most past studies (12%–17%), this foreshock rate density is close to the global foreshock rate density estimate of 8% for strike-slip earthquakes from Reasenber (1999). This makes sense as the majority of mainshocks in Southern California are strike-slip (Chen & Shearer, 2016). Our type A foreshock rate density is 35% because our mainshock magnitude is four, our minimum cut-off magnitude is 3 (making the denominator unity), and so our foreshock rate estimate and foreshock rate density are equal. This higher type A foreshock rate density (35%) compared to the classic studies (12%–17%) may be due to their use of different spatiotemporal windows, and improvements in seismic network detection in the decades since these studies.

In practice the forecasting utility of foreshocks is limited by the false detection rates. Type A foreshocks do not consider how often $M \geq 3$ earthquakes occur that are not followed by mainshocks. Type B foreshock definitions consider increases in the earthquake count that do not lead to mainshocks in the past year but no further. van den Ende and Ampuero (2020a) estimated a ~50% false positive rate for their Gamma Inter-Event Time definition. They did this by calculating the amount of time in the year prior to mainshocks where the 20-day earthquake count is above the 99th percentile of their Gamma Inter-Event Time definition (for each mainshock), which they found to be 16% of the time. They interpreted this to mean that for their finding that 33% of mainshocks have foreshocks, around half (48%) of these mainshocks with foreshocks should have been expected by chance ($16\%/33\% = 0.48$). We note that some of this time above threshold may be caused by relatively poor calibration of the Gamma Inter-Event Time definition (by effective smoothing through resampling and re-fitting Gamma distributions), compared to what we observe empirically.

We briefly assess the potential utility of type A and B foreshocks by calculating the fraction of time spent in alarm in the year prior to mainshocks. For type A, we set a 20-day alarm when a $M \geq 3$ earthquake occurs. For type B, we set a 20-day alarm when the earthquake count in the past 20 days exceeds the 99th percentile of the corresponding distribution (Empirical Seismicity Rate, Gamma Inter-Event Time, and Background Poisson). We calculate time fractions in alarm of 8% for type A, 3% for Empirical Seismicity Rate, 5% for Gamma Inter-Event Time, and 31% for Background Poisson. The Empirical Seismicity Rate definition therefore spends less than half

as much time in alarm compared to type A, at the cost of a lower hit rate (24% hit rate for the Empirical Seismicity Rate definition vs. 33% for type A).

We do not attempt more detailed analysis of type A and B foreshock forecasting utility in this study due to the retrospective nature of the work. For example, we select events within a 10 km radius of where we know a mainshock occurs, and we use 1-year of past data to calibrate type B definitions. A prospective analysis would require developing fully prospective algorithms, which is beyond the scope of this study. We note that the retrospective time fractions spent in alarms we calculate are likely minimas, and that prospective uses of type A and B foreshocks would likely lead to higher alarm time fractions. This would be due to the inclusions of regions with M3+ earthquakes, or high earthquake counts, which did not host mainshocks, and were therefore not included in our study.

5.4. Limitations

The limitations of our study (and of some previous studies) include the somewhat arbitrary nature of the parameters used in mainshock selection and foreshock definitions, including the 20-day foreshock window, the 10 km radius, the mainshock magnitude threshold of M4, and the fixed and magnitude-dependent timescales of our Combined mainshock selection method. Trugman and Ross (2019) performed a sensitivity analysis of the Magnitude-Dependent method parameters, and found that the number of mainshocks selected in the low completeness magnitude region can change by ± 2 –3 mainshocks, which can change foreshock rate estimates by ± 1 –5%. van den Ende and Ampuero (2020a) performed a sensitivity analysis on the foreshock window (changed from 20 days to 5) and found that 24% of mainshocks had foreshocks, which is in line with estimates using a 20-day window (Table 1). Although the results do not appear dependent upon the parameters, there is currently no clear physical justification for the space-time parameters used in mainshock selection or foreshock definitions, except for the space-time windows of the Magnitude-Dependent method, which are based on rupture length magnitude scaling (Wells & Coppersmith, 1994). The methods presented here reflect an empirical approach to finding foreshocks, and in the case of type B foreshocks, to identifying anomalously high seismic rates prior to relatively isolated earthquakes (mainshocks). As such, the identified foreshocks might provide some insights into the mechanisms that generate the foreshocks and perhaps the mainshock. Further research may be able to find physical justifications for these parameters, as well as a physical explanation for why $\sim 25\%$ of mainshocks have foreshocks.

5.5. Preferred Method

We found the following methods to be best practice in estimating foreshock rates:

- We select mainshocks using the Combined aftershock exclusion method, and note that there are alternative methods that could also prevent aftershocks from being selected as mainshocks.
- We use the QTM 12 catalog (inside the SCSN reporting region), because it is more complete than the SCSN catalog (Figure 1c), but contains fewer false detections than the QTM 9.5 catalog (Moutote et al., 2021; Ross et al., 2019).
- We estimate completeness magnitudes locally around mainshocks and remove earthquakes below completeness, to avoid potential biases in template-based detection manifesting as foreshocks (although we present no evidence to support a bias).
- We prefer to use the type B (high earthquake counts in foreshock windows relative to past counts) Empirical Seismicity Rate foreshock definition because it spends half as little time fraction in alarm than type A ($M \geq 3$ earthquakes in foreshock windows), 3% versus 8%, respectively, at the cost of a lower hit rate, 24% versus 33%, respectively. We note that depending on the intended use, future studies may prefer the type A definition due to the higher hit rate, at the cost of a higher time fraction in alarm. Further reasons for choosing the Empirical Seismicity Rate definition over the Gamma Inter-Event Time definition are that it does not underestimate low seismicity rates (see Section 4.2), or require assumptions for mainshocks with a lack of calibration data but clear foreshock activity (Section 3.4).

Using our preferred methodology we find 20 out of 74 mainshocks in Southern California have foreshocks (27% - Figure 11). This is similar to the previous estimate of 22% made by van den Ende and Ampuero (2020a) using the Empirical Seismicity Rate definition and Fixed aftershock exclusion to select mainshocks in the QTM 12 catalog, but for more mainshocks (74 vs. 46), and with a magnitude cut-off applied to ensure quality-controlled data. We

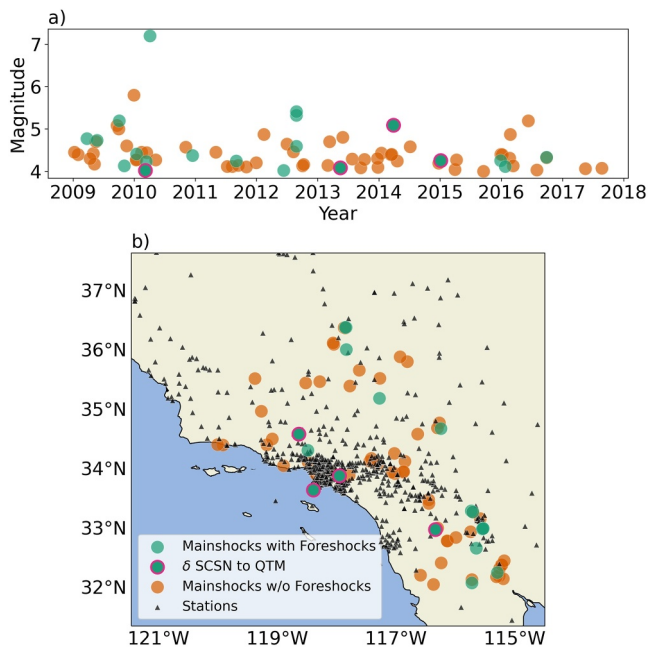


Figure 11. Times and locations of mainshocks in our merged catalog, colored by foreshock occurrence defined by type B Empirical Seismicity Rates with a magnitude cut-off applied. (a) Filled circles showing the time and magnitude of mainshocks. (b) Map of mainshock locations in the QTM 12 catalog. Teal dots denote mainshocks with foreshocks, and a pink outline denotes the four mainshocks with foreshocks in the QTM 12 but not in the SCSN. Orange dots denote mainshocks without foreshocks. Black triangles denote SCSN seismic stations with three components which were active during the entirety of the QTM catalog time span (2008–2017).

only show an increase from 46% to 51% from the SCSN to QTM catalogs. Our results therefore contradict the view that we observe type B foreshocks before significantly more mainshocks in catalogs with lower completeness magnitudes.

- Our type A ($M \geq 3$ earthquakes in foreshock windows) and B (high earthquake counts in foreshock windows relative to past counts) foreshock rate estimates differ (35% vs. 20%–30%, respectively), with our type A estimate lower than previous estimates (44%–48%). We calculate time fractions in alarm of 8% for type A foreshocks, and 3% for our preferred type B foreshock definition (the Empirical Seismicity Rate). The Empirical Seismicity Rate definition therefore spends less than half as much time in alarm compared to type A, at the cost of a lower hit rate (24% for the Empirical Seismicity Rate definition vs. 33% for type A).

The practical applications of our work include the code we publish for all mainshock selection methods and foreshock definitions used in this study, making it easy for future studies to build on our work. Our study advances the knowledge of foreshock occurrence in high resolution catalogs, but tempers the expectation that further catalog enhancement will lead to foreshock detection before significantly more mainshocks.

Data Availability Statement

The catalogs used in this study are accessible through SCEDC (2013) (Southern California Seismic Network catalog) and Ross et al. (2019) (QTM catalog).

All of the code used to generate the work in this paper is publicly available. To aid future research, we provide Jupyter notebooks which recreate all the work in this study (Azad Khan et al., 2024a), which requires the `statseis` Python module (Azad Khan et al., 2024b).

note that there are nine $M \geq 5$ mainshocks in our catalog, and five of them have foreshocks (55%) according to our preferred methodology. However, this is not a large enough sample for statistical significance (odds ratio: $M \geq 5$ mainshocks are 4.2 times more likely to have foreshocks, 99% confidence intervals 0.6 to 27.5).

6. Conclusions

In this paper we quantify how different method choices, namely mainshock selection, catalog, and foreshock definition, affect foreshock rate estimates in Southern California. We achieve this by comparing foreshock rates estimated using two mainshock selection methods, three earthquake catalogs, and four foreshock definitions.

- We analyze more mainshocks (74 vs. 53 and 46) compared to previous foreshock studies of the QTM catalog by expanding the geographical region.
- We show that mainshock selection can change foreshock rate estimates by $\pm \sim 20\%$. The Fixed and Magnitude-Dependent aftershock exclusion methods both select some aftershocks of El Mayor-Cucapah as mainshocks, and including these events impacts foreshock rate estimates.
- We introduce a new Combined mainshock selection method, which prevents aftershocks of the 2010 M7.2 El Mayor-Cucapah earthquake from being selected as mainshocks, and is more suited to regions or time periods with large $M \geq 7$ earthquakes and associated aftershocks.
- We estimate similar foreshock rates in the SCSN (20%–23%) and QTM catalogs (23%–30%) using the Empirical Seismicity Rate and Gamma Inter-Event Time definitions (with or without a magnitude cut-off). This contradicts the previously reported increase from 48% to 72% made using the Background Poisson definition without a magnitude cut-off. Our estimates for the Background Poisson definition using a magnitude cut-off

Acknowledgments

R. Azad Khan is supported by a NERC GW4+ Doctoral Training Partnership studentship from the Natural Environmental Research Council. M. J. Werner received funding from the European Union's Horizon 2020 research and innovation program under grant agreement No 821115, Real-Time Earthquake Risk Reduction for a Resilient Europe (RISE, <http://www.rise-eu.org/home/>), and by the United States Geological Survey (USGS) EHP grant G24AP00059. J. Biggs and M. J. Werner are funded by the NERC Centre for the Observation and Modelling of Earthquakes, Volcanoes and Tectonics (COMET, <http://comet.nerc.ac.uk>), a partnership between UK Universities and the British Geological Survey. J. Biggs is also funded by a Leverhulme Prize (PLP-2018-362), and ERC grant: MAST, Grant agreement ID: 101003173. A. Fagereng is supported by the project ASPERITY, selected by the ERC and funded by UKRI Frontier Research Grant Ref. EP/Y024672/1. We would like to thank Robert Churchill and Sacha Lapins for providing code for estimating the magnitude of completeness using the b-value stability method.

References

Abercrombie, R. E., & Mori, J. (1996). Occurrence patterns of foreshocks to large earthquakes in the western United States. *Nature*, 381(6580), 303–307. <https://doi.org/10.1038/381303a0>

Agnew, D. C., & Jones, L. M. (1991). Prediction probabilities from foreshocks. *Journal of Geophysical Research*, 96(B7), 11959–11971. <https://doi.org/10.1029/91JB00191>

Azad Khan, R., Werner, M., Biggs, J., & Fagereng, A. (2024b). Statseis [Software]. *Zenodo*. <https://doi.org/10.5281/zenodo.14051949>

Azad Khan, R., Werner, M., Biggs, J., & Fagereng, A. (2024a). Code for effect of mainshock selection, earthquake catalog and definition on foreshock rate estimates in southern California [Software]. *Zenodo*. <https://doi.org/10.5281/zenodo.14055540>

Cao, A., & Gao, S. S. (2002). Temporal variation of seismic b-values beneath northeastern Japan island arc. *Geophysical Research Letters*, 29(9), 48-1. <https://doi.org/10.1029/2001GL013775>

Cattania, C., & Segall, P. (2021). Precursory slow slip and foreshocks on rough faults. *Journal of Geophysical Research: Solid Earth*, 126(4). <https://doi.org/10.1029/2020JB020430>

Chen, X., & Shearer, P. M. (2016). Analysis of foreshock sequences in California and implications for earthquake triggering. *Pure and Applied Geophysics*, 173(1), 133–152. <https://doi.org/10.1007/S00024-015-1103-0/FIGURES/14>

Dodge, D. A., Beroza, G. C., & Ellsworth, W. L. (1996). Detailed observations of California foreshock sequences: Implications for the earthquake initiation process. *Journal of Geophysical Research*, 101(B10), 22371–22392. <https://doi.org/10.1029/96JB02269>

Gomberg, J. (2018). Unsettled earthquake nucleation. *Nature Geoscience*, 11(7), 463–464. <https://doi.org/10.1038/s41561-018-0149-x>

Hainzl, S. (2006). Estimating background activity based on interevent-time distribution. *Bulletin of the Seismological Society of America*, 96(1), 313–320. <https://doi.org/10.1785/0120050053>

Hauksson, E., Stock, J., Hutton, K., Yang, W., Vidal-Villegas, J. A., & Kanamori, H. (2011). The 2010 Mw 7.2 El mayor-cucapah earthquake sequence, Baja California, Mexico and Southernmost California, USA: Active seismotectonics along the Mexican pacific margin. *Pure and Applied Geophysics*, 168(8–9), 1255–1277. <https://doi.org/10.1007/S00024-010-0209-7/FIGURES/11>

Hauksson, E., Yang, W., & Shearer, P. M. (2012). Waveform relocated earthquake catalog for southern California (1981 to june 2011). *Bulletin of the Seismological Society of America*, 102(5), 2239–2244. <https://doi.org/10.1785/0120120010>

Helmstetter, A., & Sornette, D. (2003). Foreshocks explained by cascades of triggered seismicity. *Journal of Geophysical Research*, 108(B10), 2457. <https://doi.org/10.1029/2003JB002409>

Hutton, K., Woessner, J., & Hauksson, E. (2010). Earthquake monitoring in southern California for seventy-seven years (1932–2008). *Bulletin of the Seismological Society of America*, 100(2), 423–446. <https://doi.org/10.1785/0120090130>

Ito, R., & Kaneko, Y. (2023). Physical mechanism for a temporal decrease of the gutenbergrichter b-value prior to a large earthquake. *Journal of Geophysical Research: Solid Earth*, 128(12), e2023JB027413. <https://doi.org/10.1029/2023JB027413>

Jones, L. (1984). Foreshocks (1966–1980) in the san Andreas system, California. *Bulletin of the Seismological Society of America*, 74(4), 1361–1380. <https://doi.org/10.1785/BSSA0740041361>

Jones, L. (1985). Foreshocks and time-dependent earthquake hazard assessment in southern California. *Bulletin of the Seismological Society of America*, 75(6), 1669–1679. <https://doi.org/10.1785/BSSA0750061669>

Jones, L., & Molnar, P. (1976). Frequency of foreshocks. *Nature*, 262(5570), 677–679. <https://doi.org/10.1038/262677a0>

Jones, L., & Molnar, P. (1979). Some characteristics of foreshocks and their possible relationship to earthquake prediction and premonitory slip on faults. *Journal of Geophysical Research*, 84(B7), 3596–3608. <https://doi.org/10.1029/JB084B07P03596>

Li, L., Wang, B., Peng, Z., Hou, J., & Wang, F. (2024). Statistical features of seismicity associated with large earthquakes on the Chinese continent between 2008 and 2019 based on newly detected catalogs. *Seismological Research Letters*, 95(3), 1701–1717. <https://doi.org/10.1785/0220230189>

Manganiello, E., Herrmann, M., & Marzocchi, W. (2023). New physical implications from revisiting foreshock activity in southern California. *Geophysical Research Letters*, 50(1), e2022GL098737. <https://doi.org/10.1029/2022GL098737>

Marshall, S., Plesch, A., & Shaw, J. (2023). SCEC community fault model (CFM) version 6.1.

McLaskey, G. C. (2019). Earthquake initiation from laboratory observations and implications for foreshocks. *Journal of Geophysical Research: Solid Earth*, 124(12), 12882–12904. <https://doi.org/10.1029/2019JB018363>

Mignan, A. (2015). The debate on the prognostic value of earthquake foreshocks: A meta-analysis. *Scientific Reports*, 4(1), 4099. <https://doi.org/10.1038/srep04099>

Mignan, A., & Woessner, J. (2012). Theme IV-Understanding Seismicity Catalogs and their Problems Estimating the magnitude of completeness for earthquake catalogs. <https://doi.org/10.5078/corssa-00180805>

Moutote, L., Marsan, D., Lengliné, O., & Duputel, Z. (2021). Rare occurrences of non-cascading foreshock activity in southern California. *Geophysical Research Letters*, 48(7). <https://doi.org/10.1029/2020GL091757>

Nakatani, M. (2020). Evaluation of phenomena preceding earthquakes and earthquake predictability. *Journal of Disaster Research*, 15(2), 112–143. <https://doi.org/10.20965/jdr.2020.p0112>

Reasenber, P. A. (1999). Foreshock occurrence before large earthquakes. *Journal of Geophysical Research*, 104(B3), 4755–4768. <https://doi.org/10.1029/1998JB900089>

Ross, Z. E., Trugman, D. T., Hauksson, E., & Shearer, P. M. (2019). Searching for hidden earthquakes in Southern California. *Science*. https://doi.org/10.1126/SCIENCE.AAW6888/SUPPL_{_}FILE/AAW6888_{_}ROSS_{_}SM.PDF

SCEDC. (2013). Southern California Earthquake Data Center [Dataset]. *Caltech*. <https://doi.org/10.7909/C3WD3XH1>

Trugman, D. T., & Ross, Z. E. (2019). Pervasive foreshock activity across southern California. *Geophysical Research Letters*, 46(15), 8772–8781. <https://doi.org/10.1029/2019GL083725>

Trugman, D. T., & Shearer, P. M. (2017). 2. GrowClust: A hierarchical clustering algorithm for relative earthquake relocation, with application to the Spanish springs and Sheldon, Nevada, earthquake sequences. *Seismological Research Letters*, 88(2A), 379–391. <https://doi.org/10.1785/0220160188>

van den Ende, M., & Ampuero, J. P. (2020a). On the statistical significance of foreshock sequences in southern California. *Geophysical Research Letters*, 47(3). <https://doi.org/10.1029/2019GL086224>

van den Ende, M., & Ampuero, J. P. (2020b). On the statistical significance of foreshock sequences in Southern California [Software]. <https://doi.org/10.6084/M9.FIGSHARE.C.4802049.V1>

van Stiphout, T., Zhuang, J., & Marsan, D. (2012). Seismicity declustering. *Community online resource for statistical seismicity analysis*. <https://doi.org/10.5078/corssa-52382934>

Wells, D. L., & Coppersmith, K. J. (1994). New empirical relationships among magnitude, rupture length, rupture width, rupture area, and surface displacement. *Bulletin of the Seismological Society of America*, 84(4), 974–1002. <https://doi.org/10.1785/bssa0840040974>

Wetzler, N., Brodsky, E. E., Chaves, E. J., Goebel, T., & Lay, T. (2023). Regional characteristics of observable foreshocks. *Seismological Research Letters*, *94*(1), 428–442. <https://doi.org/10.1785/0220220122>

Wetzler, N., Lay, T., & Brodsky, E. E. (2023). Global characteristics of observable foreshocks for large earthquakes. *Seismological Research Letters*. <https://doi.org/10.1785/0220220397>